

The Facial Integument of Centrosaurine Ceratopsids: Morphological and Histological Correlates of Novel Skin Structures

TOBIN L. HIERONYMUS,^{1,2*} LAWRENCE M. WITMER,¹ DARREN H. TANKE,³
AND PHILIP J. CURRIE⁴

¹Department of Biomedical Sciences, Ohio University College of Osteopathic Medicine, Athens, Ohio

²Department of Biological Sciences, Ohio University, Athens, Ohio

³Royal Tyrrell Museum of Palaeontology, Drumheller, Alberta, Canada

⁴Department of Biological Sciences, University of Alberta, Edmonton, Alberta, Canada

ABSTRACT

The horned dinosaur *Pachyrhinosaurus* possesses rugose bony bosses across the skull roof in lieu of the projecting bony horn cores seen in most ceratopsians. This elaboration of typical ceratopsian ornaments provides an opportunity to test hypotheses of ceratopsian facial skin morphology and function. We analyze bone morphology and histology associated with several classes of skin features in extant amniotes using a classification tree analysis. We isolate key osteological and histological correlates for unpreserved skin structures, including both a pattern of pitting and resorption characteristic of muskox (*Ovibos*) frontal horn boss, and a pattern of metaplastic ossification characteristic of rhinoceros nasal horn boss. We also describe correlates for other skin features, such as epidermal scales and horn sheaths. Dermatocranial elements from centrosaurine ceratopsians are then examined for the same osteological and histological correlates. From this comparison we propose that the rugose bosses that replace horn cores in many centrosaurine dinosaurs, most notably *Achelousaurus* and *Pachyrhinosaurus*, were covered by a thick pad of cornified skin derived from the caudodorsal side of the primitive horn sheath comparable to the horny boss of extant muskoxen (*Ovibos*). We examine extant taxa with skin morphologies similar to *Pachyrhinosaurus* for consistent adaptive relationships between structure and behavior. We determine that high-energy head-butting is consistently associated with the acquisition of thick cornified pads, seen in muskoxen as well as helmeted hornbills [*Buceros* (= *Rhinoplax*) *vigil*] and African buffalo (*Syncerus*). The association of the bony ornaments of *Pachyrhinosaurus* with risky agonistic behaviors casts doubt on the role of species recognition as a primary selection pressure driving the diversity of all ceratopsian horns. We conclude that social selection (a broad form of intraspecific competition) is a more appropriate explanation for the diversity of centrosaurine ceratopsian

Grant sponsor: National Science Foundation; Contract grant numbers: NSF IBN-0343744, IOB-0517257; Grant sponsors: Jurassic Foundationpi, Ohio University.

*Correspondence to: Tobin L. Hieronymus, Department of Anatomy and Neurobiology, Northeastern Ohio Universities College of Medicine and Pharmacy, Rootstown, OH 44272. Fax: 330 325-5916. E-mail: h.tobin@gmail.com

Received 9 June 2009; Accepted 9 June 2009

DOI 10.1002/ar.20985

Published online in Wiley InterScience (www.interscience.wiley.com).

ornaments in the Late Cretaceous. *Anat Rec*, 292:1370–1396, 2009. © 2009 Wiley-Liss, Inc.

Key words: Centrosaurinae; *Pachyrhinosaurus*; *Ovibos*; papillary horn; social selection

INTRODUCTION

Ceratopsian dinosaurs are well known for the elaborate bony ornaments that adorn their skulls, which include a variety of projecting spikes and flanges, as well as a broad bony frill. The similarity between some of these ornaments and the horns of bovid artiodactyls (goats, sheep, antelope, and cattle) is so striking that one of the first specimens of *Triceratops* to be found was originally classified as a form of bison (“*Bison alticornis*,” Marsh, 1887). The strong similarity between the horns of ceratopsians and bovids has led to several interpretations of ceratopsian paleobiology that employ bovids as extant analogs (Farlow and Dodson, 1975).

In addition to bovid-like horns, some adult centrosaurine ceratopsians show an alternate morphology, in which the horn core is partially or wholly replaced by a rugose boss of bone. For example, the nasal horn cores of adult *Pachyrhinosaurus* spp. (Sternberg, 1950; Currie et al., 2008), *Achelousaurus horneri* (Sampson, 1995) and the Dinosaur Provincial Park pachyrhinosaur (Ryan et al., in press) are preserved as hypertrophied rugose bosses (Fig. 1). Whereas there are robust explanations for the evolution and growth of bovid-like horn cores in ceratopsids (Brown and Schlaikjer, 1940; Sampson et al., 1997; Goodwin et al., 2006; Horner and Goodwin, 2006), explanations for the formation of rugose bosses have been problematic.

This departure from typical ceratopsian horn core morphology seen in derived centrosaurines provides the opportunity to describe broader patterns of evolutionary change in ceratopsian bony ornamentation. Several functions have been proposed for ceratopsian horns, including intraspecific competition (Farlow and Dodson, 1975), sexual selection (Sampson et al., 1997), and species recognition (Padian et al., 2004; Goodwin et al., 2006), and each of these functions has a different expected evolutionary pattern (Darwin, 1871; West-Eberhard, 1983; Padian et al., 2004). The transition between projecting horn cores in *Centrosaurus* and pronounced, rugose bosses in *Pachyrhinosaurus* allows a comparison of expected and observed evolutionary patterns within Neoceratopsia.

Morphological Hypotheses for *Pachyrhinosaurus* Facial Skin

The two most prominent hypotheses for unpreserved skin structures in *Pachyrhinosaurus* spp. both place heavily keratinized (cornified) skin over the rugose surfaces of the skull. Sternberg’s (1950) initial assessment of the pitted nasal boss of *Pachyrhinosaurus canadensis* suggested a thin covering of cornified skin (Fig 2C). This hypothesis has been retained by later studies (Farlow and Dodson, 1975; Sampson et al., 1997), but an appropriate extant analog for this morphology has not

been suggested. A second hypothesis places a large, rhinoceros-like keratinous horn on the nasal and supraorbital bosses of *Pachyrhinosaurus* (Fig. 2B; Currie, 1989; Currie et al., 2008). This hypothesis draws on rhinoceros horn attachment as an extant analog, pointing to similarity between the pitted morphology seen in *Pachyrhinosaurus* and the nasal bosses of extant rhinoceros such as *Ceratotherium* and *Diceros* and the extinct rhinocerotid *Elasmotherium*. This morphological similarity was first noted on *Pachyrhinosaurus* cf. *P. canadensis* (Langston, 1967; but see also Currie et al., 2008). Aside from these explicitly stated hypotheses of integumentary morphology, a form of anatomical pachyostosis (disordered hypertrophic bone growth, distinct from histological pachyostosis as defined by Francillon-Vieillot et al., 1990) similar to that seen in muskoxen has been suggested for *Pachyrhinosaurus* skulls (Kaiser, 1960; Langston, 1975), but no skin structures were inferred based on this similarity.

Analogy and the Function of Centrosaurine Cephalic Ornaments

The morphological similarity of some ceratopsian ornaments to the horn cores of bovid artiodactyls has been used as a basis for inferring analogous horn-related behaviors, such as horn locking, clashing, and head-butting (Farlow and Dodson, 1975; Molnar, 1977; Farke, 2004). Horn-locking during intraspecific aggression also occurs in species of *Chamaeleo* with pronounced facial horns, such as *Chamaeleo jacksoni* (Bustard, 1958). In contrast, the large rugose bosses of *Achelousaurus* and *Pachyrhinosaurus* spp. are open to a broad range of functional interpretations. Sternberg (1950) suggested that the nasal boss of *Pachyrhinosaurus* and its associated skin were used as a battering ram. Farlow and Dodson (1975) suggested a similar function, comparing the nasal boss of *Pachyrhinosaurus* to the enlarged prefrontal and frontal scales of marine iguanas *Amblyrhynchus* which are used in shoving matches (Eibl-Eibesfeldt, 1966). These interpretations favor sexual or social selection as driving factors (Darwin, 1871; West-Eberhard, 1983).

In contrast, Currie et al. (2008) have suggested that the nasal and supraorbital bosses of *Pachyrhinosaurus* may have functioned predominantly as visual display structures. This may be true for either of the two suggested skin reconstructions, but a tall, rhinoceros-like horn would provide a highly conspicuous visual signal. Horn function in extant rhinoceros varies by species. For example, in black rhinoceros (*Diceros bicornis*), horn size is related to intrasexual dominance, and horns are directly used in male-male aggression (Berger and Cunningham, 1998), but similar variation in horn size has no effect on dominance or fight outcome in Indian rhinoceros (*Rhinoceros unicornis*; Dinerstein, 1991). Using

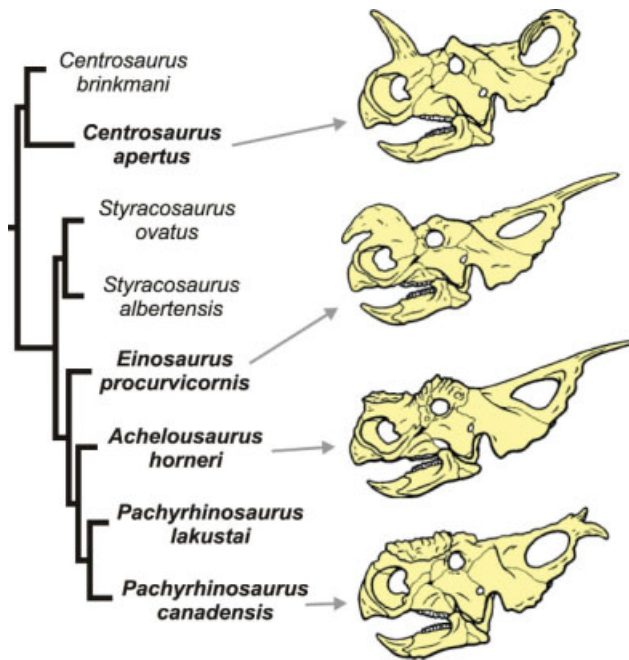


Fig. 1. Skull morphology and phylogenetic relationships of derived centrosaurine dinosaurs. Topology after Currie et al. (2008). Taxa included in this study are marked in bold.

extant rhinoceros horns as an analog for horns in *Pachyrhinosaurus* would thus not exclusively support either species recognition or sexual selection, but the possibility of tall horns as a visual display, coupled with sexual monomorphism, would favor species recognition as the driving factor in ceratopsian horn evolution (Padian et al., 2004).

Extant Analogs and Adaptation

Because a bovid or rhinocerotid analogy for ceratopsians horns addresses the function of horns in relation to their morphology, it implicitly addresses adaptation in both systems as well. Specifically, the choice of an extant analog for *Pachyrhinosaurus* implies that in both extant and extinct forms (a) the morphologies were shaped by natural selection, and (b) the process of selection entailed selection for the function of interest, not just selection of a given morphology (Sober, 1984). The “fit” of any extant analog, and thus the assessment of function in the extinct taxon, only extends as far as the testable relationship between structure and function in the extant system.

Following Gould and Lewontin’s (1979) critique of inductive studies of adaptation, tests of adaptive hypotheses have become increasingly stringent, and most currently accepted tests for adaptive explanations call for data that fossil organisms cannot provide (e.g., Reznick and Travis, 1996; Sinervo and Basolo, 1996). But even in the absence of data on performance and heritability, the evolutionary history of potentially related morphological traits can be tested for conditions sufficient for adaptive explanations, using the phylogenetic comparative tests proposed by Gould and Vrba (1982), Greene (1986), Coddington (1988), and Baum and

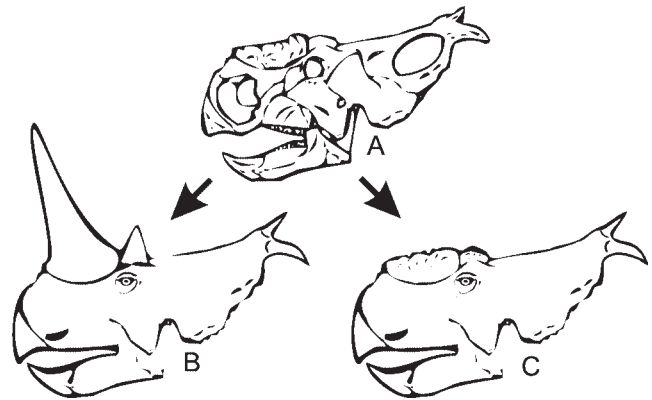


Fig. 2. The two most prominent hypotheses proposed for skin structures associated with the rugose nasal and supraorbital bosses of *Pachyrhinosaurus* (A). One hypothesis (B) places tall epidermal horns, similar to those of living rhinoceros, on the rugose patches of bone. The second hypothesis (C) places a comparatively thin covering of cornified skin on the same structures.

Larson (1991). Although these tests cannot be considered comprehensive (Grandcolas and d’Haese, 2003; Kluge, 2005), they are currently the only objective means to weigh and reject hypotheses of adaptation in extinct taxa.

Hypotheses Tested in This Study

The two most prominent hypotheses of integumentary structures described (a flat keratinous pad and a rhinoceros-like horn) are supplemented by several other morphological hypotheses in this study (Fig. 3). The additional hypotheses represent combinations of different integumentary tissues. Some of these combinations are represented by structures in extant taxa that have not previously been suggested as analogs for *Pachyrhinosaurus* horns (e.g., hornbill casques), whereas other combinations are not represented by any extant taxa (e.g., thick armor-like dermis with a thin cornified sheath), but still represent plausible morphologies for a novel structure that cannot be ruled out *a priori*. Because the morphology of *Pachyrhinosaurus* nasal bosses has been proposed as an adaptation for high-energy headbutting (Sternberg, 1950) extant analogs for novel centrosaurine horn morphologies will also be tested for behavioral correlations and adaptive relationships.

MATERIALS AND METHODS Osteological Correlates of Known Skin Structures

Because ceratopsid horn cores and bosses are novel structures that have no direct homologs in extant taxa [an extant phylogenetic bracket (EPB) level III inference per Witmer, 1995], we compared these structures to convergent structures in extant taxa to address structural and functional relationships. A diverse group of extant amniotes comprising 96 specimens from 84 taxa was sampled to test relationships between skin structures and underlying bone morphology (Table 1). Convergent examples of similar skin structures among extant taxa

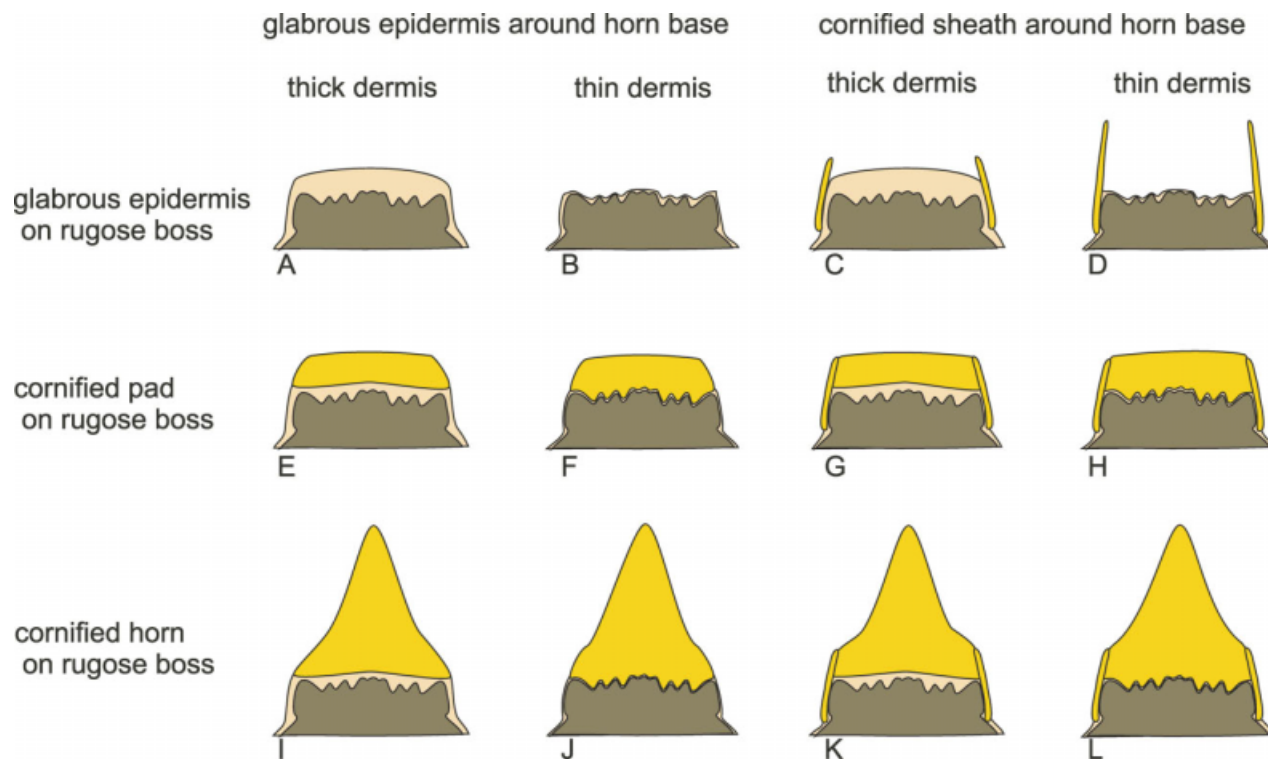


Fig. 3. Multiple working hypotheses of centrosaurine facial skin structure, using a schematic cross-section of the nasal boss of *Pachyrhinosaurus* as an example. The twelve hypotheses shown here are permutations of possible skin morphologies. The two most prominent hypotheses are shown by (H) and (I), and are similar to skin fea-

tures on extant muskoxen (H) and rhinoceros (I), respectively. Other hypotheses are similar to skin features found in extant taxa, such as suids (A) and hornbills (D), while some of the hypotheses (J) do not have extant equivalents.

were sought where available to account for phylogenetic effects.

The degree of relationship between specific types of skin structures and underlying bone morphology in extant taxa was examined by a classification tree analysis (Breiman et al., 1984; Feldesman, 2002). Representative small areas (~4 cm²) of skin from the sampled taxa were grouped into one of eight categories (Table 2) using data taken from dissections, preserved specimens, and published accounts. The corresponding bone surface beneath each sampled skin area was identified on a separate skeletal specimen of the same taxon, and the surface morphology of the underlying bone was described by six categorical variables (Fig. 4). Using a classification tree technique (recursive partitioning analysis: RPA; available in the JMP 7.0 statistical software package, SAS Institute, Cary, NC), we tested the broad skin categories for strong associations with bone morphology. RPA is a robust analysis that plays a role similar to discriminant function analysis in testing for differences among predefined groups by a set of predictor variables, the key differences being that RPA can accommodate categorical variables as well as continuous variables, and does not require that the predictor variables meet assumptions of normality or homoscedasticity.

JMP's recursive partitioning analysis makes use of logworth (log₁₀ of a weighted *p* value) to select split variables. Logworth values of 1.3 and 0.7 correspond to weighted *P* values of 0.05 and 0.2, respectively, and

these values were used as cutoffs to prevent overfitting the RPA to the data. RPA is not intended to function as a hypothesis-testing statistic in this study, but instead provides an objective means of exploring relative strengths of association between several predictor variables and a response variable in a coded morphological data set. The predictor-response relationships recovered in RPA at a logworth of greater than 1.3 are used here as robust osteological correlates of specific skin features. Relationships with a logworth between 0.7 and 1.3 will be included as noteworthy, but less robust, osteological correlates of specific skin features. In addition, some of the skin categories assigned in this study were represented by relatively few extant taxa (e.g., thickened, armor-like dermis, represented in RPA by only three extant taxa). Although skin structures with poor representation such as these are not likely to be isolated by significant splits in RPA, their osteological correlates are qualitatively different from those of other skin categories, and they will be included as less robust osteological correlates of specific skin features.

Centrosaurine Morphology

Osteological correlates of skin structures were examined on specimens of *Pachyrhinosaurus* spp., *Achelousaurus horneri*, *Einiosaurus procurvicornis*, and *Centrosaurus* spp. for morphological convergence with extant taxa (Table 3). Specimens of *Chasmosaurus belli*,

Anchiceratops ornatus, and *Protoceratops andrewsi* were included as outgroups for character polarization.

Histological Sampling

Histological samples of bone and corresponding skin were prepared from several extant taxa (see Table 4 for a list of specimens and their preparation protocols). Samples including bone and all adjacent soft tissues were taken from fixed and/or frozen specimens. These samples were dehydrated in ethanol, then infiltrated, and embedded with polymethylmethacrylate (PMMA) resin using a protocol modified from Sterchi and Eurell (1989). Additional samples of bone with known skin associations were taken from osteological specimens. Bone samples without adjacent skin were embedded in low-viscosity epoxy resin (Epo-Thin[®], Buehler, Lake Bluff, IL). All embedded samples were rough-cut on a high-speed tile saw, then serially sectioned using a variable speed diamond wafering saw (Isomet 1000[®], Buehler, Lake Bluff, IL) at 800 μm intervals. The resulting sections were mounted on cast acrylic slides with cyanoacrylate glue, then ground and polished to a thickness of $\sim 100\mu\text{m}$ on a lapidary wheel (Metaserv 2000[®], Buehler, Lake Bluff, IL).

Several cored samples of *Pachyrhinosaurus lakustai* were available from a previous histological study on this taxon (Edwards and Russell, 1994). These samples were subjected to micro-computed tomography (μCT) with a GE eXplore Locus Small Animal μCT Scanner to produce an archival record of their morphology prior to sectioning (see Table 5 for samples). Fossil samples were embedded in Silmar 41 polystyrene resin. Sectioning protocol was nearly identical to that given for extant specimens, the only exceptions being that the fossil samples were serially sectioned at 1mm intervals and mounted to glass slides using epoxy resin.

Testing Hypotheses of Adaptation and Analogy

After examples of convergent skin morphology between centrosaurines and extant taxa were identified, hypotheses of analogy were tested in three steps: (1) the strength of any relationships between function and skin morphology was assessed by checking how often similar functions occurred among morphologically convergent extant taxa; (2) extant taxa showing similarity in both function and skin morphology from step 1 were examined in phylogenetic context to test for adaptation in the sense of Gould and Vrba (1982); (3) inferred skin morphologies for centrosaurines were examined in phylogenetic context to test for similarity between the adaptive phylogenetic histories identified in step 2 and the character transformation history inferred for centrosaurine skin structures.

The first step, assessing the strength of functional relationships to skin morphology in extant taxa, is ideally carried out as a quantitative character correlation test that accounts for phylogeny, such as the Discrete test found in the BayesTraits software package (Pagel, 1994; Pagel and Meade, 2006). However, comparing diffuse phylogenetic distributions of convergent morphologies (e.g., comparing horn sheaths on the frontal horns of bovids and the tarsometatarsal spurs of galloanserine birds) can strain the assumptions of these tests, particularly the assumptions

of complete representation of a phylogenetic tree and known branch lengths. In cases where phylogenetic comparative tests of character correlation were impractical, contingency table tests such as χ^2 were employed to test relationships between structure and function instead. Both of these approaches test the hypothesis that a specific function co-occurs with a specific skin morphology more often than would be expected by random chance. Significant non-random relationships between structure and function are suggestive of adaptation (although not a complete test for adaptation *per se*; see Kluge, 2005), especially if such relationships occur homoplastically in several phylogenetically independent groups (Greene, 1986). This first test will hereafter be referred to as the “convergence” test of analogy.

The second step, examining structure/function relationships in phylogenetic context, was performed by calculating ancestral character state reconstructions of the relevant morphological and functional characters in Mesquite v2.5 (Maddison and Maddison, 2006, 2008). Published phylogenies for extant taxa identified as morphologically convergent with centrosaurines in step 1 were imported into Mesquite. Morphological and functional (behavioral) traits were coded as categorical characters from osteological data and published descriptions. Both maximum parsimony (MP) and maximum likelihood (ML) methods of ancestral character state reconstruction were used. Branch length information was taken from published phylogenies where available; otherwise, ML ancestral character state reconstructions were run once with all branch lengths equal (modeling punctuated change) and once each with Grafen’s (1989) and Pagel’s (1992) methods of transforming branch lengths to model gradual change.

Ancestral character state reconstructions for skin morphology and function allowed these characters to be tested against Gould and Vrba’s (1982) phylogenetically explicit definition of adaptation, as suggested in Codrington (1988, 1990) and Baum and Larson (1991). Because appropriate fitness or performance data for specific skin morphologies are rarely available, this part of the three-part test for analogy focused on the “historical genesis” of skin morphology in extant taxa (Gould and Vrba, 1982) in relationship to the selective regime of specific functions or behaviors. Skin morphology/function relationships identified in step 1 were only considered as appropriate extant analogs if the convergent morphology and a novel function arose on the same branch; i.e., if the structure/selective regime relationship matched a specific subset of Gould and Vrba’s (1982) historical definition of adaptation (Fig. 5A). There are more inclusive definitions of “adaptation” that are not covered by this pattern [i.e., the evolution of novel structure after a change in selection regime (Fig. 5B), or the pattern of exaptation in which a novel selection regime follows the evolution of a novel structure (Fig. 5C)]. It is also still unclear whether change in selection regime and morphological change are more often tightly related (Fig. 5A) or whether change in morphology is expected to lag behind change in selection regime (Fig. 5B; viz. Larson and Losos, 1996). However, of these two patterns, the arrangement shown in Fig. 5B is more likely to occur by random chance. For this reason, and because fitness data were not available for most morphologies considered in this study, lagging patterns of potentially

TABLE 1. Taxa sampled for RPA

Taxon	Specimen numbers	Sample area
<i>Aceros undulatus</i>	UMMZ 153059, UMMZ 154514	Frontal, premaxillae
<i>Alces alces</i>	OUVC 9559	Nasal
<i>Alligator mississippiensis</i>	OUVC 9638	Premaxilla
<i>Anhima cornuta</i>	SMF 2479	Cornual process
<i>Anseranas semipalmata</i>	UMMZ	Frontal casque
<i>Anthracoseros malabaricus</i>	CM 11699	Dentary
<i>Balaenoptera physalus</i>	Senckenberg exhibit	Maxilla
<i>Basiliscus basiliscus</i>	UMMZ 128120	Nasals
<i>Bison bison</i>	OUVC 9489	Nasal, os cornu
<i>Buceros bicornis</i>	UMMZ 219874	Dentary
<i>Buceros hydrocorax</i>	UMMZ 207467	Caudal casque
<i>Bycanistes brevis</i>	UMMZ 158192	Parietals
<i>Bycanistes bucinator</i>	CM 14946, CM 14912	Maxilla, dentary
<i>Castor canadensis</i>	OUVC 9532	Nasal, unguis
<i>Casuarius unappendiculatus</i>	UMMZ 220266	Frontal casque
<i>Catharacta skua</i>	CM 10116	Parietals
<i>Ceratogymna fistulator</i>	CM 15918	Premaxillae
<i>Cerorhinca monocerata</i>	CM 5119, CM 8126	Caudal nasals, premaxillae
<i>Chamaeleo cf. C. jacksoni</i>	UMMZ 154065, UMMZ 151087	Frontals, nasal horn
<i>Chauna torquata</i>	UMMZ 156989	Phalangeal spur
<i>Chlamydosaurus kingii</i>	UMMZ 210540	Lacrimal
<i>Choloepus sp.</i>	MOR OST 320	Frontals
<i>Choriotis kori</i>	UMMZ 205539	Dentary
<i>Cochlearius cochlearius</i>	CM 16303	Premaxillae
<i>Cordylus giganteus</i>	UMMZ unkn	Epiparietal osteoderm
<i>Corucia zebrata</i>	UMMZ 189832	Nasals
<i>Corytophanes cristatus</i>	UMMZ 129890, UMMZ 148961	Frontals, nasals
<i>Crax rubra</i>	UMMZ 70027	Dentary
<i>Cyclura cornuta</i>	UMMZ 149033, UMMZ 128581	Postorbital, nasals
<i>Cyclura ricordi</i>	UMMZ 149036	Nasals
<i>Cygnus olor</i>	ROM 155840	Frontal casque
<i>Daption capense</i>	UMMZ 224214, UMMZ 224212	Lacrimal, premaxillae
<i>Diomedea antipodensis</i>	SMF 2093	Premaxillae
<i>Elgaria multicaarinata</i>	UMMZ 188741	Frontal osteoderm
<i>Enyalioides laticeps</i>	UMMZ 149071	Frontals
<i>Equus hemionus</i>	OUVC 9706	Dorsal unguis
<i>Eudiptes chrysolophus</i>	CM 11198	Frontals
<i>Eudiptula minor</i>	UMMZ 213082	Premaxillae
<i>Eurypyga helias</i>	UMMZ 209158	Premaxillae
<i>Fratercula corniculata</i>	UMMZ 134436	Parietals
<i>Fulmarus glacialis</i>	CM 13892	Dentary
<i>Gekko gekko</i>	UMMZ 127664	Frontals
<i>Gerrhosaurus major</i>	UMMZ 174415	Osteoderms
<i>Giraffa camelopardalis</i>	MNHN 1985-201	Median ossicone
<i>Halobaena caerulea</i>	CM 8444	Premaxillae/maxilla
<i>Heloderma horridum</i>	UMMZ 181151	Osteoderms
<i>Hippopotamus amphibius</i>	MNHN 1943-27	Premaxilla
<i>Hylchoerus meinertzhageni</i>	USNM 308851	Jugal
<i>Iguana iguana</i>	UMMZ 149093	Nasals
<i>Laemanctus serratus</i>	UMMZ 149101	Frontals
<i>Macroneustes giganteus</i>	CM 11040	Frontals
<i>Malaclemys terrapin</i>	OUVC 9805	Shell
<i>Moloch horridus</i>	UMMZ 210529	Postorbital
<i>Nyctibius grandis</i>	UMMZ 208949	Premaxillae
<i>Oceanites oceanicus</i>	CM 4909	Parietals
<i>Ovibos moschatus</i>	ROM CN 1148, USNM RS18S176	Frontal boss
<i>Pachyptila turtur</i>	UMMZ 211550	Frontals
<i>Pachyptila vittata</i>	UMMZ 216167, UMMZ 215019	Frontals, maxilla
<i>Pelecanoides urinatrix</i>	UMMZ 213094, UMMZ 224220	Parietals, premaxillae
<i>Pelecanus erythrorhynchus</i>	ROM 151169	Breeding crest attachment
<i>Penelopides panini</i>	CM 11551, CM 12499	Parietals, premaxillae
<i>Phacochoerus aethiopicus</i>	OUVC 9491	Nasal
<i>Phalacrocorax auritus</i>	CM 7358, CM 422	Frontals, premaxillae
<i>Phrynosoma cornuta</i>	UMMZ 149116	Parietal horn
<i>Pinguinus impinnis</i>	CM 8273	Premaxillae
<i>Pogona vitticeps</i>	OUVC 9734	Maxilla
<i>Psophia leucoptera</i>	UMMZ 211514	Premaxillae

TABLE 1. Taxa sampled for RPA (Continued)

Taxon	Specimen numbers	Sample area
<i>Sarkidiornis melanotos</i>	ROM 120525	Premaxillae/Nasals
<i>Sceloporus poinsetti</i>	UMMZ 189465	Nasals
<i>Sternotherus minor</i>	OUVC 10604	Frontal, maxilla
<i>Sula dactylatra</i>	UMMZ 220885	Premaxillae
<i>Sus scrofa</i>	OUVC 9473	Nasal, dorsal ungual
<i>Tapirus indicus</i>	MNHN 1944-267	Nasals
<i>Terrapene carolina</i>	OUVC 10605	Shell, maxilla
<i>Tetracerus quadricornis</i>	MNHN 1927-18	Frontal Horn
<i>Tiliqua rugosa</i>	UMMZ 128109	Osteoderm
<i>Tiliqua scincoides</i>	UMMZ 203418	Osteoderm
<i>Tinamus major</i>	UMMZ 70019	Premaxillae
<i>Tockus erythrorhynchus</i>	CM 2274	Maxilla
<i>Tragulius napu</i>	USNM 49871	Frontals
<i>Ursus americanus</i>	OUVC 9562	Nasal
<i>Varanus exanthematicus</i>	OUVC 9735	Maxilla
<i>Varanus salvator</i>	UMMZ 168411	Maxilla
<i>Xema sabinii</i>	UMMZ 223721	Dentary

Each taxon contributed a maximum of two data points to the analysis.

Institutional abbreviations: CM, Carnegie Museum; MNHN, Muséum nationale d’Histoire naturelle; MOR OST, Museum of the Rockies osteology collection; OUVC, Ohio University Vertebrate Collection; ROM, Royal Ontario Museum; SMF, Forschungsinstitut Senckenberg; UMMZ, University of Michigan Museum of Zoology; USNM, Smithsonian National Museum of Natural History.

TABLE 2. Skin categories for recursive partitioning analysis (RPA)

Skin category	Examples
Villose skin	Typical mammalian pelage (i.e., fur)
Feathered skin	Avian plumage (i.e., feathers)
Glabrous skin	Soft skin with few or no epidermal appendages
Cornified sheaths	Horns of bovid artiodactyls; horny beaks of birds and turtles
Epidermal scales	Scales and cephalic shields of turtles, squamates, and crocodylians
Projecting skin structures	Epidermal horns of rhinoceros; breeding crests of American white pelicans (epidermal) and comb ducks (dermal)
Armor-like dermis	Thickened dermis of rhinoceros, hippopotamus, and swine

adaptive morphological change (Fig. 5B) and patterns of exaptation (Fig. 5C) were rejected as analogs, as these patterns could not be distinguished from nonaptation without evidence of current utility. Changes in skin morphology that occurred on the same branch as changes in function in ancestral character state reconstructions were retained as potential extant analogs for centrosaurine morphology. This second test will hereafter be referred to as the “aptation” test of analogy.

The third step, comparing the “historical genesis” of convergent morphology in potential extant analogs to the pattern of horn evolution in centrosaurine dinosaurs, was accomplished by comparing the ancestral character state reconstructions from step 2 with MP and ML ancestral character state reconstructions for centrosaurine horn morphology. Inferred skin morphologies for centrosaurine dinosaurs were coded as categorical characters, using categories similar to those used for the potential extant analogs. The centrosaurine phylogeny of Currie et al. (2008) was imported into Mesquite v2.5. Equal branch lengths (modeling punctuational change) and branch length

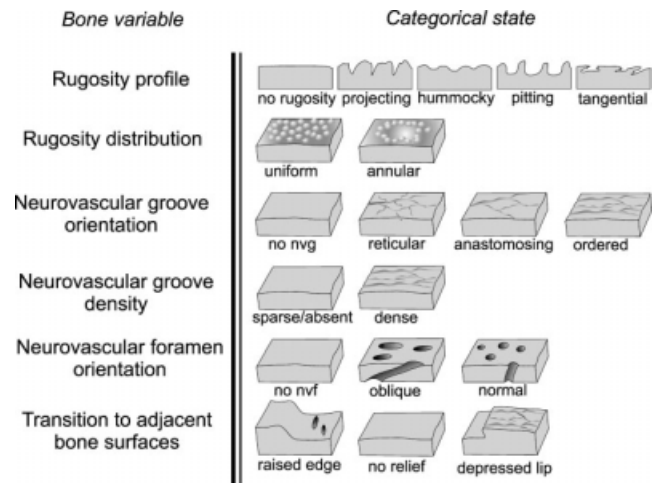


Fig. 4. Schematics for categorical variables used to describe bone surfaces in this study (rows), with examples of the states for each variable. Schematics for rugosity type show the surface profile in cross-section; other schematics show the surface and profile of a small (2 × 2 cm²) sample area. Nvf, neurovascular foramina; nvg, neurovascular grooves.

transformations of Grafen (1989) and Pagel (1992), both modeling gradual change, were included in ML ancestral character state reconstruction analyses.

Similarity in the “historical genesis” of morphological traits among extant and extinct groups, as determined from ancestral character state reconstructions, is the third and final criterion in our test of analogy. Morphological traits in extant taxa were considered to represent analogous structures for centrosaurine morphology only if the sequence of character state changes leading to both extant and extinct morphologies were similar (Fig. 6). Two independent lineages will not necessarily respond to a similar selective regime by producing

TABLE 3. Centrosaurine specimens and outgroups examined for gross osteological correlates

<i>Achelousaurus horneri</i>	MOR 485, MOR 571, MOR 591
<i>Anchiceratops ornatus</i>	ROM 802
<i>Anchiceratops</i> sp.	AMNH FR 5251
Centrosaurinae indet.	ROM 49862
<i>Centrosaurus apertus</i>	ROM 12776, ROM 767, TMP 1966.33.17
<i>Centrosaurus</i> sp.	ROM 831
cf. <i>Centrosaurus</i>	AMNH FR 5442, ROM 12782, ROM 12787, ROM 43214, ROM 49863, ROM 636, ROM 641, ROM 728, TMP 1992.36.224
<i>Centrosaurus</i> cf. <i>C. apertus</i>	TMP 1987.18.20, TMP 1989.18.148
<i>Chasmosaurus belli</i>	ROM 839
<i>Einiosaurus procurvicornis</i>	MOR 373a, MOR 373b, MOR 373c, MOR 456a, MOR 456b, MOR 456c, MOR 456d, MOR 456e
<i>Pachyrhinosaurus</i> cf. <i>P. canadensis</i>	Drumheller skull, ^a UCMP 88H8-4-4
<i>Pachyrhinosaurus lakustai</i>	TMP 1985.112.1, TMP 1985.112.28, TMP 1986.55.102, TMP 1986.55.155, TMP 1986.55.206, TMP 1986.55.258, TMP 1987.55.110, TMP 1987.55.156, TMP 1987.55.228, TMP 1987.55.304, TMP 1987.55.320, TMP 1987.55.323, TMP 1987.55.81, TMP 1989.55.1009, TMP 1989.55.1111, TMP 1989.55.1112, TMP 1989.55.1125, TMP 1989.55.1131, TMP 1989.55.1185, TMP 1989.55.1234, TMP 1989.55.1396, TMP 1989.55.1524, TMP 1989.55.172, TMP 1989.55.172, TMP 1989.55.188, TMP 1989.55.21, TMP 1989.55.203, TMP 1989.55.207, TMP 1989.55.256, TMP 1989.55.367, TMP 1989.55.427, TMP 1989.55.467, TMP 1989.55.561, TMP 1989.55.566, TMP 1989.55.566, TMP 1989.55.566, TMP 1989.55.72, TMP 1989.55.781, TMP 1989.55.918, TMP 1989.55.927; TMP 1989.55.931, TMP 1989.55.958
<i>Protoceratops andrewsi</i>	AMNH FR 6429

Museum abbreviations: AMNH FR, Am Mus of Natural History Fossil Reptiles; MOR, Museum of the Rockies; ROM, Royal Ontario Museum; TMP, Royal Tyrrell Museum of Palaeontology; UCMP, University of California Museum of Paleontology.

^aThis specimen, described in Langston (1967), was studied from a cast housed in the collections of the Royal Tyrrell Museum of Palaeontology.

TABLE 4. Extant histological specimens

Taxon	Specimen no.	Location	Tissues sampled
<i>Colaptes auratus</i>	OUVV 10400	Premaxilla and rictus	Bone and soft tissue
<i>Corvus brachyrhynchus</i>	OUVV 10403	Premaxilla and rictus	Bone and soft tissue
<i>Gerrhosaurus major</i>	OUVV 10410	Premaxilla and maxilla	Bone and soft tissue
<i>Hemitheconyx caudicinctus</i>	OUVV 10411	Premaxilla and maxilla	Bone and soft tissue
<i>Larus delawarensis</i>	OUVV 10399	Premaxilla and rictus	Bone and soft tissue
<i>Lepidophyma flavimaculatum</i>	OUVV 10418	Premaxilla and maxilla	Bone and soft tissue
<i>Oplurus cuvieri</i>	OUVV 10419	Premaxilla and maxilla	Bone and soft tissue
<i>Megascops asio</i>	OUVV 10402	Maxillary rostrum	Bone and soft tissue
<i>Phalacrocorax auritus</i>	OUVV 10401	Premaxilla and rictus	Bone and soft tissue
<i>Varanus exanthematicus</i>	OUVV 10414	Premaxilla, maxilla, dentary	Bone and soft tissue
<i>Ceratotherium simum</i>	OUVV 9541	Nasal horn, frontal horn	Bone and soft tissue
<i>Giraffa camelopardalis</i>	OUVV 10513	Median ossicone	Bone and soft tissue
<i>Ovibos moschatus</i>	UAM 86916	Frontal horn boss	Bone and horn sheath
<i>Crocodylus porosus</i>	OUVV 10576	Maxilla	Bone
<i>Alligator mississippiensis</i>	OUVV 9633	Maxilla	Bone
<i>Chrysemys picta</i>	OUVV unnumbered	Maxilla	Bone and horny beak

Institutional abbreviations: OUVV, Ohio University Vertebrate Collection; UAM, University of Alaska Museum of the North.

similar adaptive changes (Kluge, 2005); thus this final criterion cannot falsify a potential analog, but may instead be used to rank hypotheses by their relative support. This third and final test will hereafter be referred to as the “correspondence” test of analogy.

RESULTS

Osteological Correlates of Skin in Extant Taxa

Cornified sheaths and scales both have osteological correlates that were identified as robust (splits at log-worth > 1.3) by RPA. Armor-like dermis, projecting skin

appendages, and thick pads of papillary epidermis were separated from cornified sheaths in a less robust split by RPA (logworth = 1.22), and although they were not split further, the osteological correlates for these three taxon-poor skin categories are qualitatively distinctive and consistent among the available samples within each taxon (Table 6). Skin morphologies with comparatively soft keratinization and nonspecialized dermal architecture (“glabrous” or soft, hairless skin, “villose” or hairy skin, and feathered skin) were separated from other skin categories by the absence of specific bony features such as neurovascular grooves or rugose bone.

TABLE 5. Paleohistological specimens

Specimen no.	Source specimen no.	Description
TMP 1993.55.2	TMP 1989.55.894	Border of bony nostril
TMP 1993.55.8	TMP 1989.55.1038	Caudal nasal boss
TMP 1993.55.9	TMP 1989.55.894	Tip of developing nasal horn core
TMP 1993.55.10	TMP 1989.55.894	Lateral surface of developing nasal horn core
TMP 1993.55.11	TMP 1989.55.174	Lateral surface of developing nasal horn core
TMP 1993.55.12	TMP 1986.55.48	Lateral surface of developing nasal horn core
TMP 1993.55.13	TMP 1987.55.161	Lateral surface of developing nasal horn core
TMP 1993.55.16	TMP 1989.55.1342	Basal sulcus of nasal boss
TMP 1993.55.17	TMP 1989.55.1342	Lateral surface of nasal boss
TMP 1993.55.18	TMP 1989.55.1342	Lateral surface of nasal adjacent to boss
TMP 1993.55.20	TMP 1989.55.1342	Basal sulcus of nasal boss

Specimens of *Pachyrhinosaurus lakustai* from the study of Edwards and Russell (1994) used in this study. All paleohistological specimens were μ CT scanned for archival record. Scan parameters were as follows: slice thickness of 92 μ m (isotropic voxels), 80 kV, 450 μ A, 100 ms, 720 views. The resulting volume data (in VFF format) were exported from MicroView 2.1.2 (open-source software developed by GE; microview.sourceforge.net) in DICOM format, which were then subsequently imported into Amira 3.1.1 or 4.1.1 (Mercury-TGS, Chelmsford, MA) for viewing, analysis, and visualization. Institutional abbreviations: TMP, Royal Tyrrell Museum of Palaeontology.

Correlates of epidermal morphology: Cornified sheath. Cornified sheaths that cover bony cores, such as the horns of bovid artiodactyls and the beaks of birds and turtles, are consistently associated with prominent neurovascular grooves on bone surfaces, in agreement with the results of Horner and Marshall (2002). Other features that are generally associated with cornified sheaths include a low profile for any rugose bone that may be present, with bone spicules directed tangentially along the bone surface; neurovascular foramina that breach the bone surface at shallow, oblique angles; and the presence of a pronounced “lip” or bony overgrowth at the transition between heavily cornified skin and adjacent soft skin (Fig. 7A). The last feature may be absent if the transition between cornified skin and soft skin is gradual, as in the horns of pronghorn antelope (*Antilocapra*), where the hardened horn sheath continues as a softer, villose “epikeras” or transitional horn which in turn merges with the surrounding villose skin of the frontal region. Estimates of type I and II error rates for this correlate in the RPA sample are shown in Table 7.

Correlates of epidermal morphology: Scales.

Epidermal scales show two distinct forms of osteological correlate, coinciding with the difference between intradermal and periosteal ornamentation noted by Vickaryous et al. (2001). The first correlate is formed by intradermal ossifications, often referred to as osteoderms or osteoscutes. Each separate ossification generally corresponds to a single overlying scale (e.g., the osteoderms of *Heloderma*), although in some cases several well-developed osteoderms may sit beneath a single epidermal scale (e.g., *Tiliqua scincoides*; *Tarentola mauritanica*, Lange, 1931, p 418). Osteoderms may co-ossify with adjacent skeletal elements in ontogenetically older individuals, but in most cases osteoderms that have fused with underlying skull bones remain identifiable as discrete elements.

A second form of osteological correlate for scales can be seen in many iguanian lizards, and consists of a regularly arranged, shallow, hummocky rugosity on the bone surface (Fig. 7B). These features are not related to intradermal ossification and are instead derived entirely from apophyseal bone growth beneath individual scales

(Vickaryous et al., 2001). In some iguanian lizards, these features become pronounced (e.g., the supraorbital and nasal horn cores of *Chamaeleo jacksoni*). Taken together, these two forms of osteological correlates produced a significant split by RPA that isolated most of the scaled specimens included in the analysis, and both of these morphologies are considered robust osteological correlates for epidermal scales in extinct taxa. Estimates of type I and II error rates for these correlates in the RPA sample are shown in Table 7.

Correlates of epidermal morphology: Cornified pad.

Thick, cornified pads of epidermis are comparatively rare and are commonly found in only three of the extant taxa surveyed in this study: helmeted hornbills (*Buceros vigil*), African buffalo (*Syncerus caffer*), and muskoxen (*Ovibos moschatus*). The morphology of the epidermis is slightly different in each case. Adults of both sexes of *Buceros vigil* possess a heavily cornified pad of “hornbill ivory” that covers the rostral end of the casque. The epidermis in this pad grows directly away from the flat face of the casque, and lacks any grossly visible internal structure. Male *Syncerus* possess a comparatively thin pad of cornified epidermis across a bony frontal boss that is continuous with the horn sheath. The epidermal tissue of both the pad and the horn sheath is organized into discrete bundles, indicating the presence of pronounced dermal papillae at the dermo-epidermal junction. Growth of the cornified pad in *Syncerus* progresses at a shallow angle with respect to the underlying bone surface, similar to growth of the horn sheath along the bony horn core. The cornified pad of male *Ovibos* is also organized in discrete bundles of papillary epidermis (in the sense of Homberger, 2001), but is much thicker than that of *Syncerus*, and grows away from the flat surface of the boss at a much steeper angle.

Adult male *Syncerus* and both sexes of *Buceros vigil* both show similar bony features beneath the thickened parts of their horns and beaks, respectively. In both cases, the bone that supports the heavily cornified pad of epidermis is highly vascular, and the bone surface itself is pierced by a dense group of normally-oriented (i.e., oriented more or less perpendicularly to the

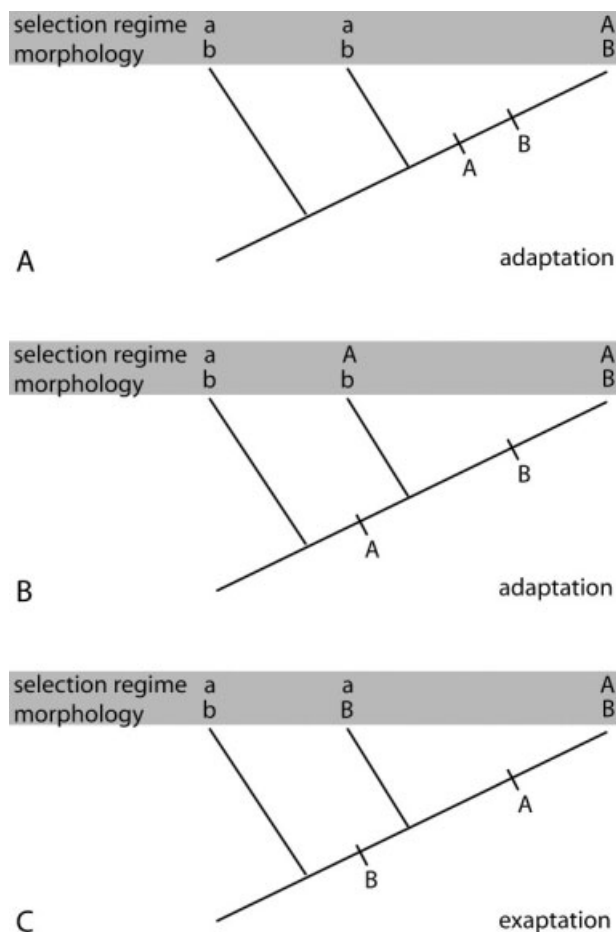


Fig. 5. Phylogenetic patterns of character state change and selection regime. **A:** Character state and selection regime change on the same branch. This pattern is one of two patterns that falls under Gould and Vrba's (1982) definition of adaptation, and the only pattern that we consider sufficient evidence for analogy in the absence of fitness data. **B:** Character state changes after change in selection regime. While this pattern also falls under Gould and Vrba's (1982) definition of adaptation, it permits varying degrees of separation between character state change and the change in selection regime. **C:** Character state change before change in selection regime. This pattern fits Gould and Vrba's (1982) definition of exaptation, and may represent a biologically meaningful relationship between structure and function, but is also expected to occur more often by random chance than pattern (A).

surface) neurovascular foramina. This correlate contrasts sharply with the oblique neurovascular foramina and neurovascular grooves seen beneath the adjacent horn sheath in *Syncerus* and the adjacent horny beak in *Buceros vigil*.

The frontal bosses of adult male *Ovibos* show a slightly different osteological correlate. In addition to dense concentrations of normally-oriented neurovascular foramina, the bone surface shows a pronounced pitted rugosity, composed of shallow rounded depressions separated by fine projecting bone spicules (Fig. 7C). Computed tomographic (CT) scans of an osteological specimen of *Ovibos* with horns in place (UAM 86916) show that the rounded depressions and projecting spi-

cles match up with the edges and centers, respectively, of individual bundles of papillary epidermis.

The frontal bosses of adult male *Ovibos* also show a pronounced depression relative to the adjacent horn core, a feature shared by Pleistocene-age woodland muskoxen *Bootherium bombifrons* (e.g., USNM 37287). This large-scale feature is distinct from the smaller-scale pitting described previously, and remains visible even after extensive post-mortem weathering has obliterated the fine-scale pitted rugosity (e.g., USNM 2555). A similar pronounced depression is found on the nasal boss of atypical individuals of Indian rhinoceros *Rhinoceros unicornis* in which the nasal horn has been worn down to a thin pad (~2-cm thick; e.g., USNM 308417). Individuals of *Rhinoceros unicornis* with typical horns (~10–15cm tall) show the distinct osteological correlate for projecting skin structures instead, described in the next section.

Correlates of dermal and epidermal morphology: Projecting skin structures. The category of projecting skin structures includes features that are composed predominantly of epidermal tissues (e.g., rhinoceros horns) or dermal tissues (e.g., the crests of male comb ducks, *Sarkidiornis*) that form horns or crests without internal bony support. Although some examples of projecting skin structures are not associated with bony correlates (e.g., the “warts” of warthogs, *Phacochoerus*), those that are show a surprisingly consistent arrangement of rugose bone, detailed in Hieronymus and Witmer (submitted for publication). The outer circumference of the projecting feature is marked by an area of rugosity formed by projecting bone lobules or spicules, which gives way to smooth bone beneath the center of the projecting feature (Fig. 7D).

Correlates of dermal morphology: Armor-like dermis. The category of armor-like dermis includes several convergent examples of a specific architecture of dermal collagen fibers (Shadwick et al., 1992). This architecture consists of regular diagonally crossed arrays of thick collagen fiber bundles arranged at oblique angles to the plane of the overlying epidermis. This arrangement contrasts with typical sauropsid dermis, in which smaller fiber bundles are diagonally crossed but lie parallel to overlying epidermis (Landmann, 1986; Sawyer et al., 1986), and also differs from typical mammalian dermis, in which smaller fiber bundles are arranged at random but lie parallel to the overlying epidermis (Sokolov, 1982). The osteological correlate for armor-like dermis consists of a rugosity formed by large (>2-mm in diameter) projecting bone lobules, each composed of metaplastically ossified remnants of collagen fiber bundles from the base of the dermis (Fig. 7E). These features are described in more detail in Hieronymus and Witmer (submitted for publication).

Histological Correlates of Skin in Extant Taxa

Histological correlates of cornified sheaths/armor-like dermis. The bony attachments of horn sheaths, horny beaks, and armor-like dermis are characterized by dense concentrations of metaplastically ossified dermal collagen fibers (extrinsic fibers) that meet

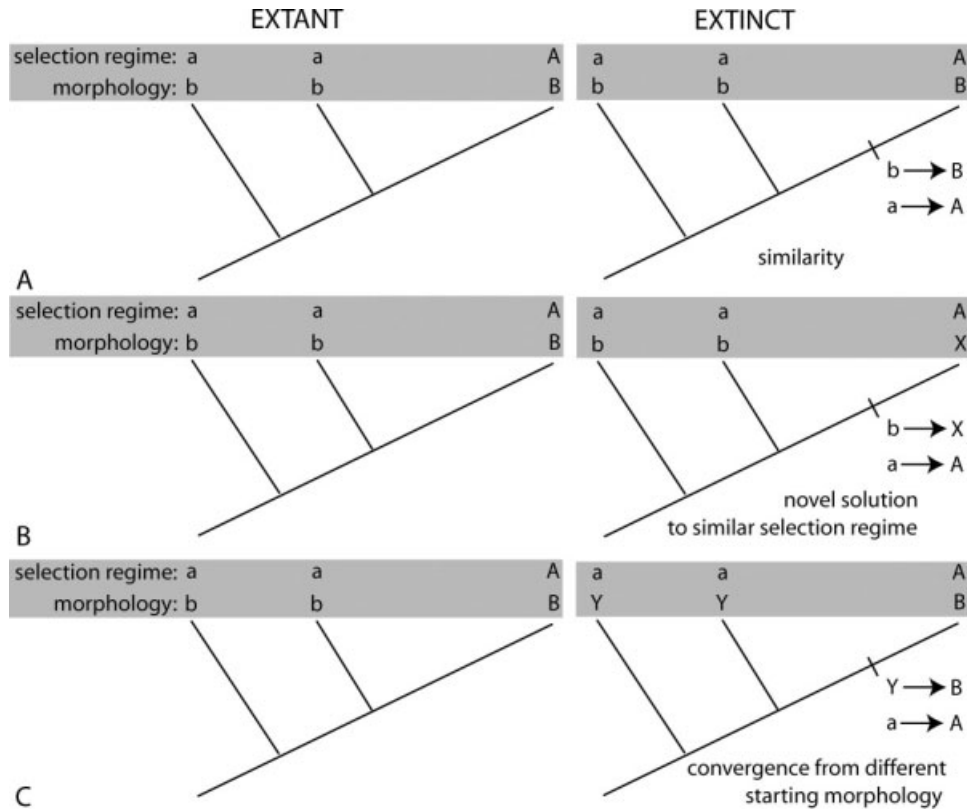


Fig. 6. Patterns of similar and dissimilar character state transformation among potential analogs. **A:** Similar transition sequences among extant and extinct taxa. This is the preferred pattern for hypotheses of analogy. **B:** Different “solutions” to similar selection regimes. This

pattern leads to a false negative in assessing function (Kluge, 2005). **C:** Convergence from different primitive morphologies. This pattern cannot falsify a hypothesis of analogy, but leads to a lower rank of preference than pattern (A).

TABLE 6. Osteological and histological correlates of skin structures

Skin structure	Example	Osteological correlates	Histological correlates
Cornified sheaths	Bovoid horn	Tangentially oriented rugosity Dense neurovascular grooves Oblique neurovascular foramina “Lip” at transition to softer skin	Dense concentrations of extrinsic fibers with low insertion angles and crossed arrays
Epidermal scales	Squamate scales	Shallow hummocky rugosity Osteoderms	Normally-oriented extrinsic fibers
Cornified pads	Muskox horn boss	Pits or elongate grooves Normal neurovascular foramina Raised edge at transition to softer skin	Bone spicules composed of osteonal bone Osteoclast lacunae
Projecting structures	Rhinoceros horn	Projecting rugosity distributed in a ring around the edge of the projecting structure	Bone spicules composed of metaplastically ossified dermis
Armor-like dermis	Hippopotamus facial skin	Evenly-distributed projecting rugosity	Bone spicules composed of metaplastically ossified dermis

the bone surface at oblique angles. In some cases (all examples of armor-like dermis, some beaks and horns) these extrinsic fibers are part of an orthogonally crossed array, whereas in others the extrinsic fibers are all oriented along a single shallow chord to the bone surface. Some beak attachments (e.g., *Megascops asio*) only show small, restricted patches of extrinsic fibers; others (e.g., *Phalacrocorax auritus*) show a continuous layer of extrinsic fiber bone across the entire attachment (Fig. 8A).

Although the dermal architecture is similar between cornified sheaths and armor-like dermis, the conformation of bony structures at the periosteal surface is different. Under cornified sheaths, metaplastic ossification of the dermis proceeds along a uniform front, producing a flat surface (Fig. 8A). This differs from the patchy ossification of dermal collagen fiber bundles in armor-like dermis that produces projecting spicules of metaplastic bone (Fig. 8E).

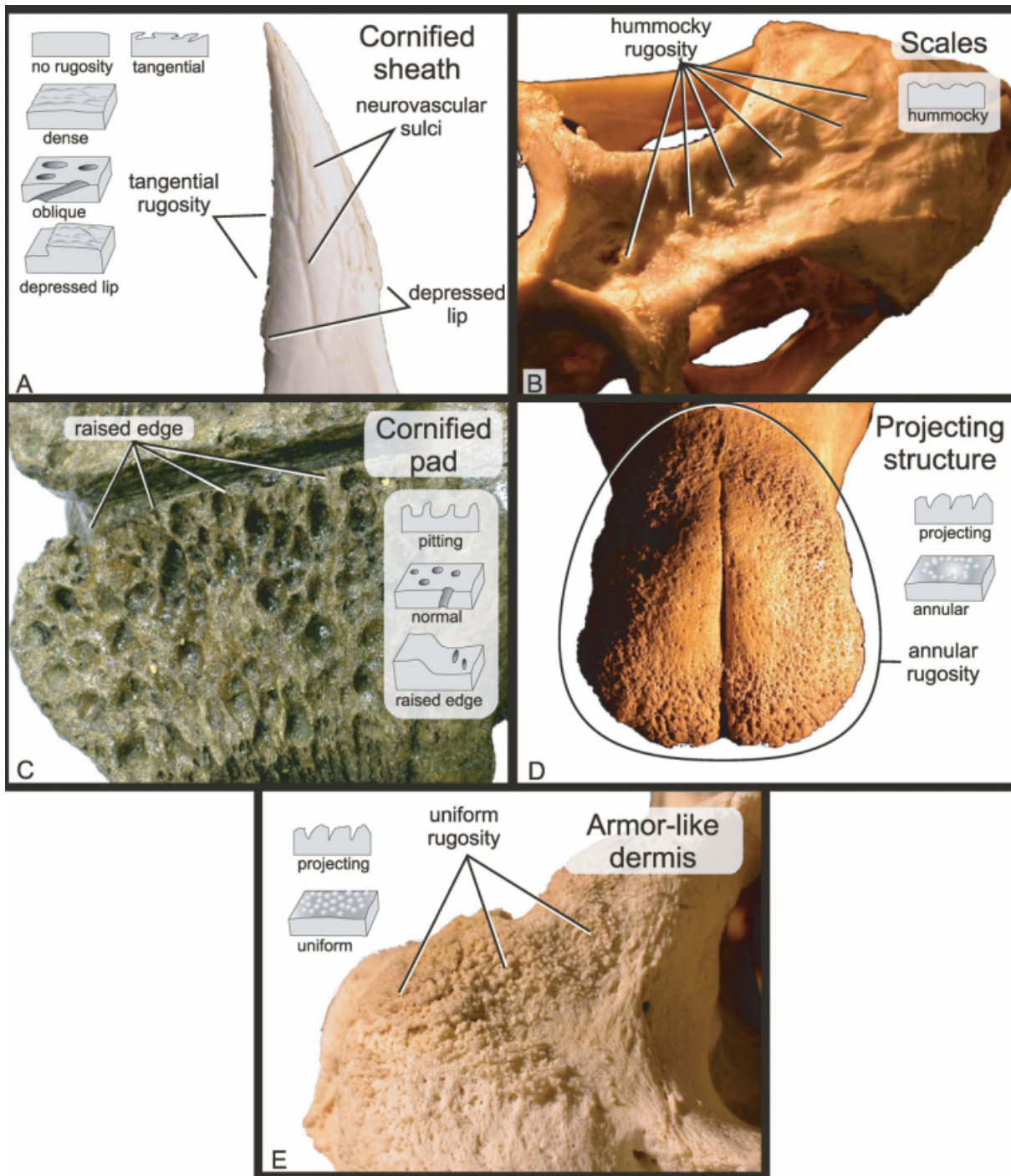


Fig. 7. Osteological correlates for categories of skin structures used in this study, represented by an example of the associated bone surface and schematics of the associated bone variable scores: **(A)** cornified sheath, shown on the metacarpophalangeal spur of a crested creamer (*Chauna torquata*, UMMZ 156989); **(B)** scales, shown on the skull roof of a green iguana (*Iguana iguana*, UMMZ 149093); **(C)** cornified pad, shown on the frontal boss of a fossil specimen of

muskoos (*Ovibos moschatus*, USNM RSFVL # 18 S. #176); **(D)** projecting skin structure, shown on the nasal boss of white rhinoceros (*Ceratotherium simum*, AMNH 81815); and **(E)** armor-like dermis, shown on the premaxilla of hippopotamus (*Hippopotamus amphibius*, USNM 313712). Villose skin, feathered skin, and glabrous skin are not associated with bony correlates.

Histological correlates of epidermal scales.
The bony attachment of epidermal scales is sometimes accompanied by extrinsic fibers, but less often than the

attachment of cornified sheaths. The extrinsic fibers that occur beneath the epidermal scales of squamates are generally oriented normal to the periosteal surface of

TABLE 7. Estimates of Type I error rate, Type II error rate, and accuracy of the two correlates identified by significant splits in recursive partitioning analysis (RPA)

Correlate set	Type I error rate	Type II error rate	Accuracy (%)
Cornified sheath	0.21	0.05	85
Epidermal scale	0.08	0.39	85

Type I error (false positive) is the probability of incorrectly classifying a bone surface as the specified category (e.g., classifying a bone surface as a cornified sheath correlate when in fact is associated with feathered skin); Type II error (false negative) is the probability of classifying a related bone surface as another category (e.g., not classifying a bone surface as a cornified sheath correlate when in fact it is associated with a cornified sheath).

the bone instead of the shallow angles seen with other skin attachment types. The apophyseal ossification that produces scale-associated hummocky rugosity in iguanian squamates (Fig. 8B) is not caused by metaplastic ossification of the dermis, and instead appears to be the result of periosteal ossification. There are generally few prominent bundles of extrinsic fibers in iguanian hummocky rugosity, and the laminar bone of the individual hummocks is continuous with adjacent dermatocranial bone.

Histological correlates of cornified pads. Of the two gross osteological correlate types associated with thick cornified pads, only the pitted morphology of muskox horn bosses was histologically examined in this study. The bony horn boss is composed of highly vascular plexiform bone, with no evidence of any extrinsic fibers. The spicules on the bone surface are outlined by osteoclast lacunae (Fig. 8D), and contain partial remnants of osteons, suggesting that the shape of the spicules is a result of the resorption of existing bone.

Histological correlates of projecting skin structures. The peripherally-distributed rugosity associated with rhinoceros horns is composed of metaplastically ossified dermal collagen fiber bundles that form projecting bone spicules (Fig. 8E; Hieronymus and Witmer, submitted for publication). The comparatively smooth central region within the peripheral rugosity is composed of periosteally ossified bone with no extrinsic fibers. The size of the projecting bone spicules in this osteological correlate closely matches the size of the large bundles of collagen fibers in the armor-like dermis of rhinoceros. The size difference in individual bone spicules between this osteological correlate in rhinoceros and the correlate for projecting structures in taxa without derived dermal architecture (e.g., *Sarkidiornis*) suggests that the peripheral rugosity in all examples of this correlate is formed by metaplastic ossification of existing dermal collagen fiber bundles.

Skin Correlates in Centrosaurines: Results and Discussion

Osteological correlates of skin in Centrosaurus. Nasal horn cores of *Centrosaurus* generally show prominent neurovascular grooves and obliquely-oriented neurovascular foramina, both of which are robust corre-

lates for the presence of a cornified sheath. Most specimens also show a “lip” or basal sulcus (“bony overgrowth” of Ryan and Russell, 2005) that describes a saddle-shaped curve at the base of the nasal horn core (Fig. 9A), indicating a transition between more heavily cornified skin on the nasal horn core itself and softer skin across other parts of the nasals.

The dorsal processes of the premaxillae and the premaxillary processes of the nasals also show evidence of a cornified cover that most likely extended ventrally across part of the bony nostril (Fig. 9E). Other areas of the nasals are generally smooth, but the combination of sparse neurovascular grooves and a broad convex curve on the caudal edge of the nasals suggests the presence of large epidermal scales.

Supraorbital horn cores of *Centrosaurus* show prominent neurovascular grooves, indicating the presence of a cornified sheath, with a basal sulcus preserved on the medial side of the major horncore in some specimens. Where present, a basal sulcus indicates a sharp transition between a horn sheath covering the horn core and softer skin medially. In some individuals, the supraorbital horn core is marked by one or two pronounced depressions on the apex of the horn. These features match the shallow pitting described by Sampson et al. (1997) and the more general phenomenon of “cranial pitting” described by Tanke and Farke (2006). The presence of a basal sulcus and pronounced neurovascular grooves associated with these depressions (e.g., ROM 12787) indicates that the adjacent areas of the supraorbital horn core were covered by a cornified sheath, and the pits themselves match the correlate for thick cornified pads seen in extant muskoxen, especially in the presence of a pronounced depression relative to adjacent parts of the horn core. The finer pitted rugosity seen in muskox horn cores is not always present in *Centrosaurus* supraorbital horn cores. The combination of a central depression and a peripheral basal sulcus suggests that the apex of the supraorbital horn core was covered by a thickened pad of cornified skin that continued around the base of the horn core as a cornified sheath. A similar arrangement of pitting and neurovascular grooves relating to a thickened distal horn and thinner proximal horn sheath can be found on the horncores of male big-horn sheep (*Ovis canadensis*; Shackleton, 1985).

The supraorbital horn core is accompanied by a series of low ridges of bone that closely match the apophyseally derived osteological correlate for scales in iguanian squamates, suggesting that the supraorbital horn itself is an evolutionary derivative of the third in a series of four scales that line the dorsal rim of the orbit (Fig. 9C). This series of scale correlates extends onto the squamosal, where there are another four to five shallow bony prominences in sequence (Fig. 9D). In some specimens (ROM 767, AMNH FR 5442) a second row of two scale correlates can be seen rostroventral to the primary row on the squamosal. A similar row of six bony prominences on the parietal is also interpreted as the correlate for a sequence of scales (Fig. 9F).

Osteological correlates of skin in Einiosaurus.

The rostrally curved nasal horn cores of adult *Einiosaurus procurvicornis* show prominent bony correlates for the presence of a cornified sheath. A basal sulcus on the

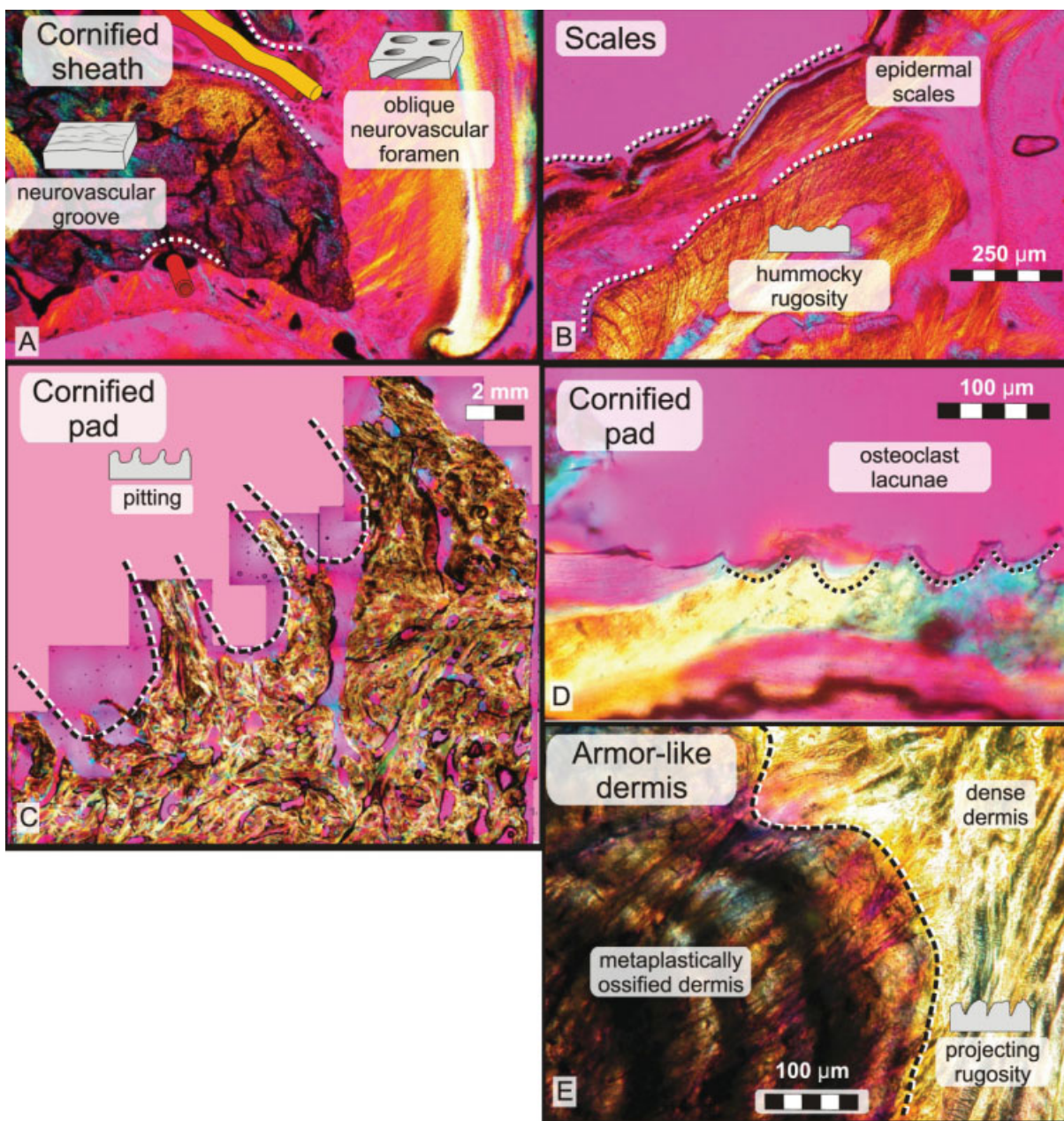


Fig. 8. Histological correlates for categories of skin structures used in this study, represented by an example histological section: **(A)** cornified sheath, shown on a coronal section from the rostrum of a double-crested cormorant (*Phalacrocorax auritus*, OUV 10401); **(B)** scales, shown on a longitudinal section from the nasals of a Madagascar spiny-tailed iguana (*Oplurus cuvieri*, OUV 10419); **(C)** and **(D)** cornified pads, shown on coronal sections from the frontal boss of a

muskox (*Ovibos moschatus*, UAM 86916); and **(E)** armor-like dermis, shown on a coronal section from the frontal of a white rhinoceros (*Ceratotherium simum*, OUV 9541). The segment of skin and bone shown on this slide is associated with the attachment of the frontal horn; similar features occur in areas without horn attachment, such as the lateral surface of the zygomatic process of the temporal bone.

nasal horn core defines a saddle-shaped lateral outline for the transition between the heavily cornified horn sheath and softer surrounding skin, similar to that seen in *Centrosaurus* (Fig. 10A,D).

Two adult nasal horn cores taken from the Canyon Bonebed site (MOR 456 8-9-6-1 and MOR 456 8-13-7-5) both show a shallow longitudinal groove along their

dorsal surfaces (Fig. 10B). This groove may have been related to a thickening of the cornified horn sheath on the dorsal surface of the horn core, but the bone surface is weathered and there are no conclusive osteological correlates for such a skin structure. The adult nasal horn core taken from the Dino Ridge site (MOR 373 8-20-6-14) lacks a dorsal longitudinal groove. Sampson

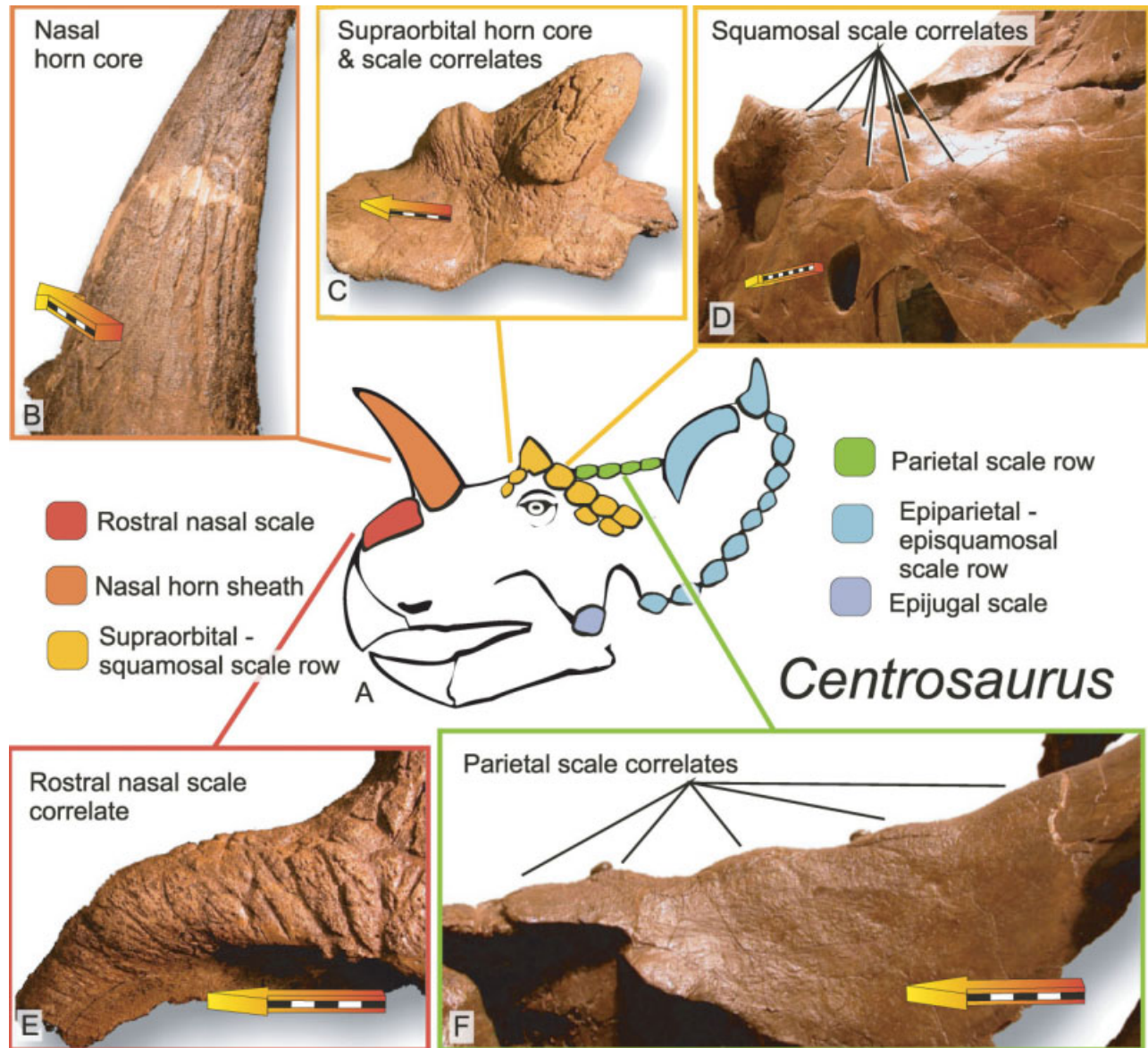


Fig. 9. **A:** Skin structures inferred for *Centrosaurus*, based on osteological correlates visible in insets (**B–F**). Scale bars are 5 cm with arrowhead pointing rostrally, unless otherwise noted. **B:** Neurovascular grooves on the nasal horn core. **C:** Basal sulcus on supraorbital horn core, caudal to a raised scale correlate. **D:** A row of shallow scale correlates on the squamosal. Scale bar is 10 cm. **E:** Neurovascular sulci and faint basal sulcus on the nasal rostral to the nasal horn core. **F:** A median row of shallow scale correlates on the parietal bar.

tal horn core, caudal to a raised scale correlate. **D:** A row of shallow scale correlates on the squamosal. Scale bar is 10 cm. **E:** Neurovascular sulci and faint basal sulcus on the nasal rostral to the nasal horn core. **F:** A median row of shallow scale correlates on the parietal bar.

et al. (1997) concluded that these grooves and similar grooves in *Centrosaurus* specimens are present in more ontogenetically mature individuals, in a manner similar to the ontogenetic distribution of cranial pitting proposed by Tanke and Farke (2006).

Supraorbital skin correlates in *Einosaurus* are similar to those seen in *Centrosaurus*. Some *Einosaurus* specimens (e.g., MOR 456 8-9-6-1) show a pronounced apical pit in the position of the supraorbital horn core, but the raised rim of bone surrounding the pit still bears a basal sulcus, indicating a thin cornified sheath at the edge of a thicker cornified pad (Fig. 10C). Bony prominences indicative of a row of scales on either side of the supraorbital

horn core are also present, although weathering and cracking in the available *Einosaurus* material makes it difficult to compare the total number of bony prominences, relative to better-preserved examples from *Centrosaurus*.

Osteological correlates of skin in *Achelousaurus*. Adult *Achelousaurus horneri* nasal horn cores show a pronounced rostral slant (Fig. 11D). This orientation differs from that seen in *Einosaurus* in that the pitch of the horn core is established at the base and remains straight, instead of curving forward. The caudodorsal surface of the horn core shows the osteological correlate

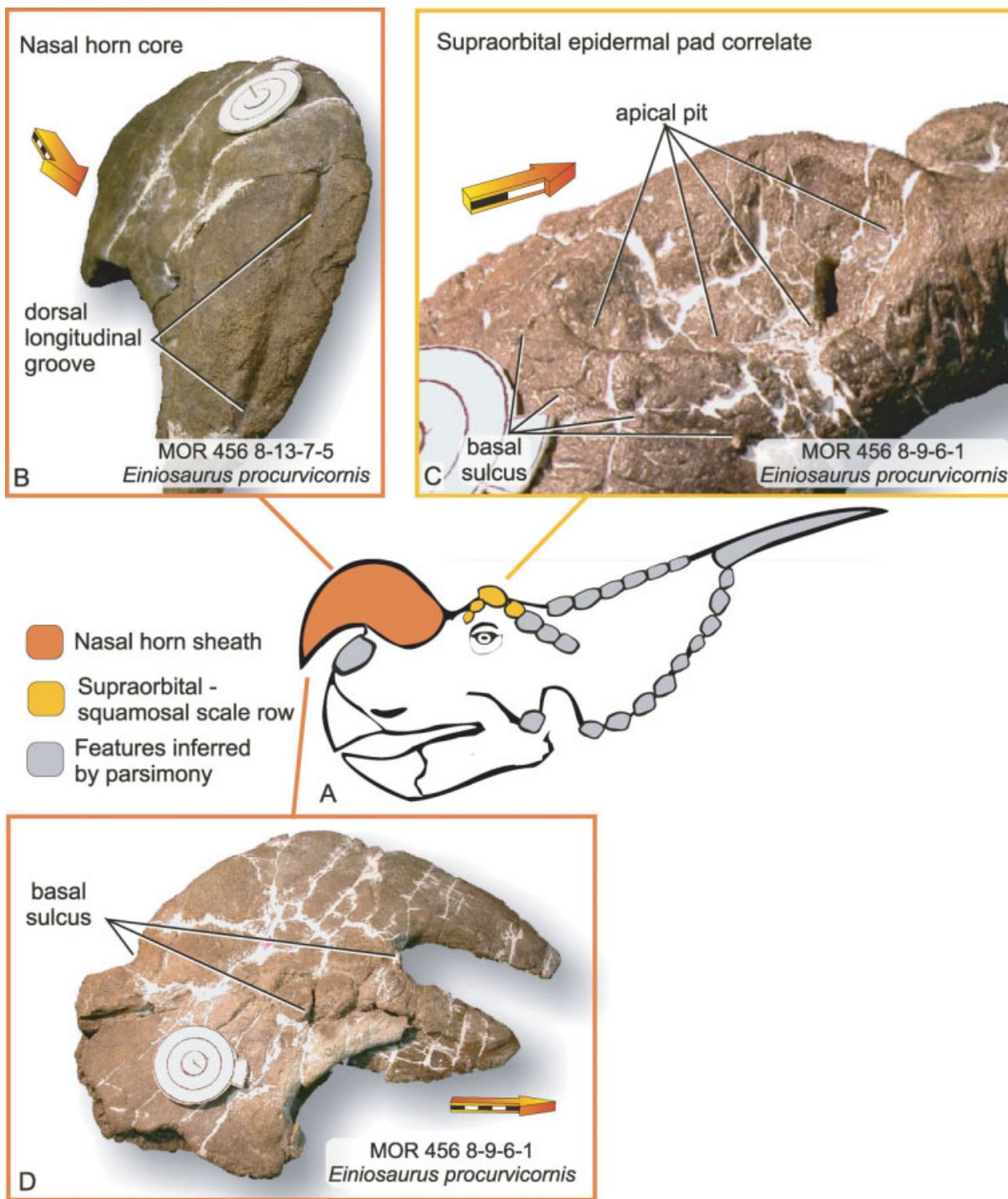


Fig. 10. **A:** Skin structures inferred for *Einosaurus*. Shaded elements were not represented by skeletal specimens in this study, and are inferred from the presence of similar structures in other centrosaurine taxa. **B:** Nasal horn core, showing dorsal longitudinal groove present in Canyon Bonebed specimens. Scale bar is 5 cm, with

arrowhead pointing rostrally. **C:** Apical pit in the place of supraorbital horncore, with a basal sulcus indicating the extent of the cornified sheath. Scale bar is 2 cm. **D:** Basal sulcus of the nasal horn core. Scale bar is 5 cm.

for a thick epidermal pad which grades into the osteological correlate for a cornified sheath laterally. Bone morphology on the dorsal surface of adult *Achelousaurus*

nasal horn cores is most similar to the grooved morphology seen at the transition between the boss and the horn core proper in muskoxen, in which thick papillary

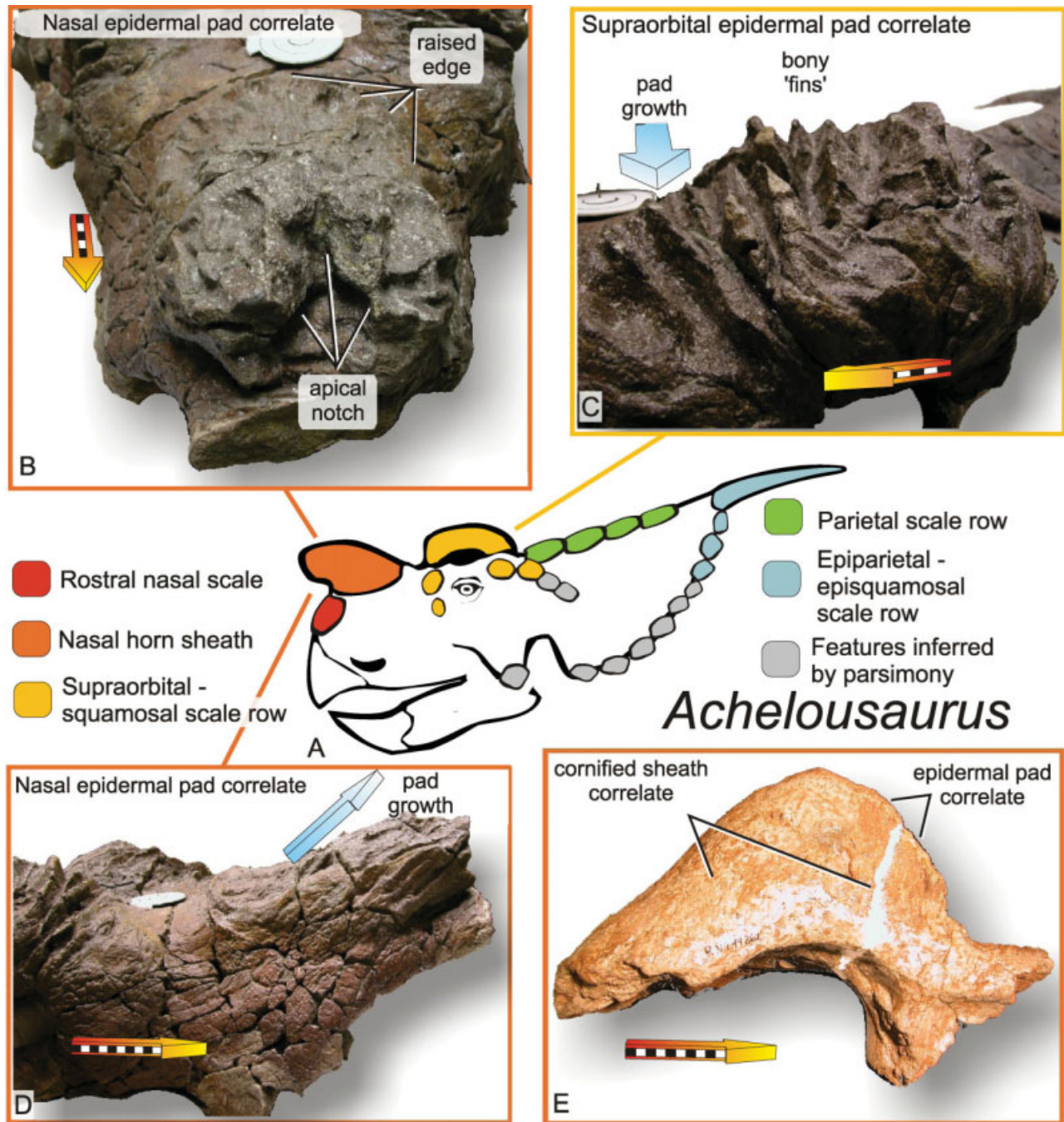


Fig. 11. **A:** Skin structures inferred for *Achelousaurus*. Shaded elements as in Fig. 10. Scale bars are 5 cm with arrowhead pointing rostrally, unless otherwise noted. **B:** Rostral view of the nasal boss, showing the apical notch with superimposed pitting. Raised edge indicates the caudal extent of the cornified nasal pad. **C:** Rostrolateral view of the supraorbital region, showing bony “fins” similar to those seen on extant muskoxen. Blue arrow indicates inferred growth direc-

tion, towards the viewer. **D:** Lateral view of nasal boss, with inferred growth direction for the cornified nasal pad. Compare with Fig. 12E. Scale bar is 10 cm. **E:** Unidentified centrosaurine nasal horn core (ROM 49862) with the osteological correlate for a cornified pad at the rostral apex. Morphology is transitional between that of *Einosaurus/Centrosaurus* and *Achelousaurus*. Scale bar is 10 cm.

epidermis grows at a low angle to the underlying bone surface, elongating the characteristic pits into shallow grooves.

The rostral (apical) end of the nasal horn core shows a deep v-shaped notch on the midline (Fig. 11B),

which may correspond to the dorsal longitudinal groove seen in the Canyon Bonebed *Einosaurus specimens*. Pitting indicative of a thick pad of rostrally-growing papillary epidermis is superimposed on this midline apical notch.

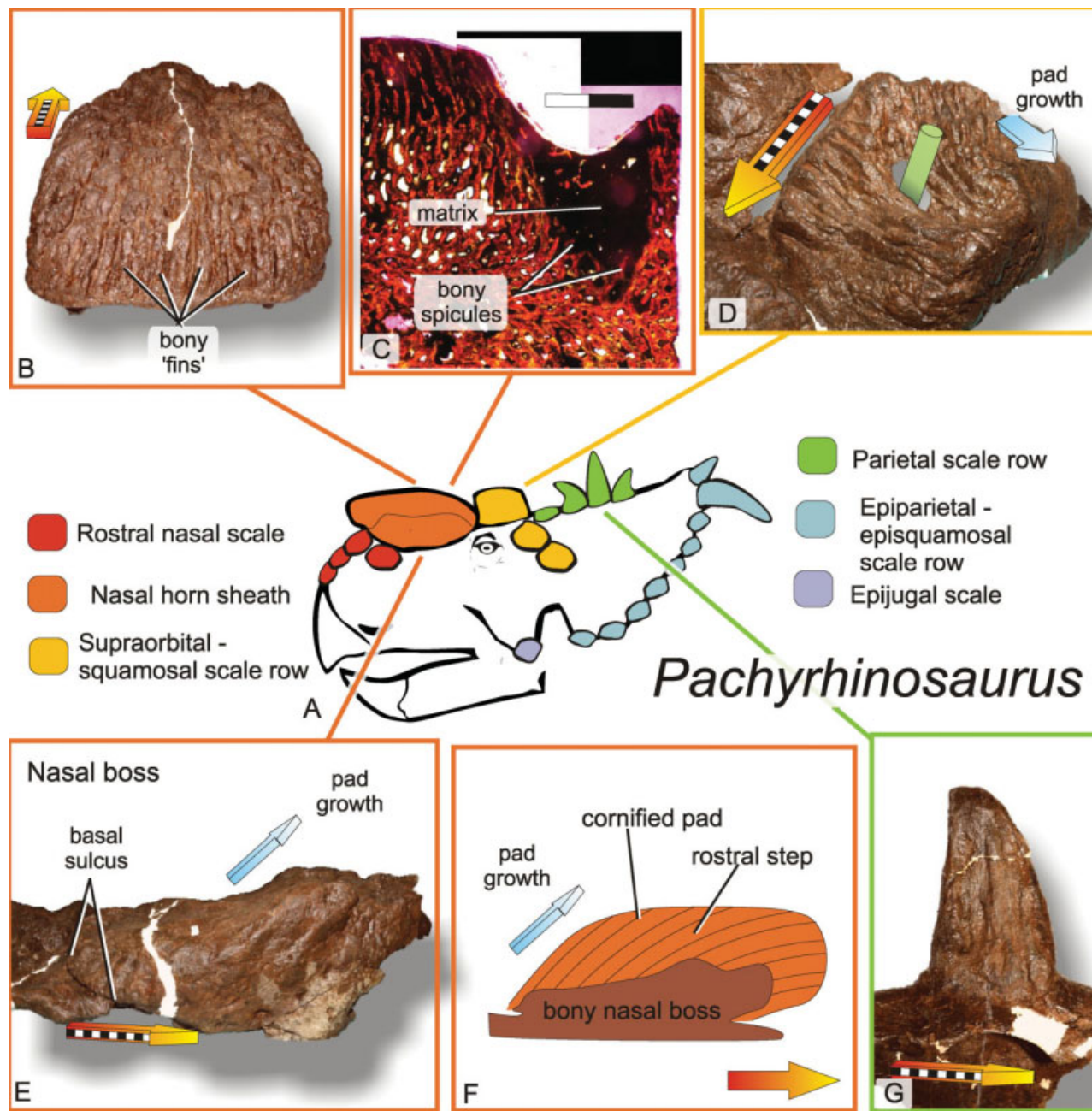


Fig. 12. **A:** Skin structures inferred for *Pachyrhinosaurus*. Scale bars are 10 cm with arrowhead pointing rostrally, unless otherwise noted. **B:** Caudal view of the nasal boss of TMP 86.55.206 *P. lakustai*, showing bony “fins” indicative of a cornified pad growing at a low angle to the bone surface. **C:** Histological section of a bony “fin” and sulcus from the nasal boss of *P. lakustai*, showing infill of matrix and fine bone spicules; compare to Fig. 8C. Scale bar is 2 mm. **D:** Supra-orbital boss of TMP 89.55.427 *P. lakustai*, showing bony “fins” and

communication with frontal sinus (green bar). Blue arrow shows inferred growth direction for the overlying cornified pad. **E:** Nasal boss of TMP 89.55.427 *P. lakustai*, showing basal sulcus and bony “fins” at the caudal end of the boss. The nasal boss of this specimen is similar to an adult *Achelousaurus* nasal boss (Fig. 11D). **F:** Schematic of inferred cornified tissue on the bony nasal boss of *Pachyrhinosaurus* spp. **G:** Parietal horn of TMP 86.55.258 *P. lakustai*.

The rostrally-slanted horn core and rostral pitting seen in *Achelousaurus* can also be seen in another unidentified centrosaurine horn core (ROM 49862; Fig 11E). This specimen shows a pronounced basal sulcus, indicating a cornified sheath covering the entire base of

the horn core, instead of the development of the caudo-dorsal side of the horn sheath into a comparatively thick pad as seen in *Achelousaurus*. This may represent a transitional morph between *Einosaurus* and *Achelousaurus*, but this specimen lacks locality data and its

stratigraphic position relative to these two taxa cannot be established.

The supraorbital bosses of adult *Achelousaurus* specimens show surface morphology that closely resembles the transition between boss and horn core proper in muskoxen, indicating a thick pad of papillary epidermis growing at a shallow angle relative to the bone surface (Fig. 11C). The direction of growth of the supraorbital epidermal pad in *Achelousaurus* can be inferred from the orientation of the “fins” of bone in the boss, suggesting a lateral direction of growth similar to that seen on the curved supraorbital horn cores of *Centrosaurus brinkmani* (Ryan and Russell, 2005). The large supraorbital boss lacks a basal sulcus, thus the supraorbital horn pad can be inferred to stop at the rostral, caudal, and medial edges of the wrinkled bone of the boss, instead of continuing around the periphery as a thin cornified sheath. This inferred skin morphology can be seen as part of a continuum with the supraorbital horn sheaths inferred for *Einosaurus* and *Centrosaurus*. Simple apical pitting occurs in cases where a cornified horn sheath remains at the periphery. More complex pitted surfaces such as those of *Achelousaurus* supraorbital bosses resemble epiphyses, and indeed may be constrained to this morphology by a similar need to attach two hardened structures together while maintaining a softer germinative layer between them.

Osteological and histological correlates of skin in *Pachyrhinosaurus*. Some examples of adult nasal bosses in *Pachyrhinosaurus lakustai* (e.g., TMP 1989.5.427) are similar to the adult nasal horn core of *Achelousaurus*, with a clearly defined apical notch, rostral pitting, and a gradation from dorsal pitting to lateral neurovascular grooves (Fig. 12E). These correlates indicate skin morphology similar to that inferred for *Achelousaurus*, with a thick pad of papillary epidermis growing rostrally across the dorsal surface of the boss and continuing rostrally from the apical notch. This heavily cornified pad grades laterally into a cornified sheath across the lateral base of the horn core. Further similarities between this morphology and the more derived structures of other specimens of *Pachyrhinosaurus lakustai* and *Pachyrhinosaurus canadensis* provide a basis for identifying homologous regions on the nasal boss in these taxa.

The variable morphology of the dorsal surface of the nasal boss in *Pachyrhinosaurus lakustai* is the result of varying degrees of post-mortem weathering and erosion (Currie et al., 2008). The osteological correlate for a thick cornified pad seen on muskoxen is relatively robust, and remains visible even after considerable weathering, as seen in Pleistocene fossil muskox specimens (e.g., USNM RSVL 18 S 176; Fig. 7C). Thus despite damage to the original bone surface, the pitting and grooving seen on *Pachyrhinosaurus lakustai* can be readily interpreted as a similar osteological correlate.

A histological specimen from the dorsal surface of the nasal boss shows that the bony pitting and grooving is more pronounced than it appears on the prepared surface of the fossil (Fig. 12C). The bottoms of the grooves in this specimen lie beneath an additional 3 mm of matrix, which preserves several fine bony spicules. Similar bone spicules were reported to have been removed

during preparation of the Drumheller *Pachyrhinosaurus* specimen, and it is these bone spicules that were specifically described as potentially similar to the rugose bone of rhinoceros horn attachment (Langston, 1967). Comparison of the bone spicules from TMP 1989.55.1038 (Fig. 12C) to histological sections of rhinoceros horn attachment (Fig. 8E) and muskox horn attachment (Fig. 8D) shows the rugose boss of *Pachyrhinosaurus* to be more similar to the frontal bosses of muskoxen on a histological level. The bone spicules of muskoxen and *Pachyrhinosaurus* are both composed of osteonal bone tissue, whereas the lobules of bone in rhinoceros horn attachment are composed of metaplastically ossified deep dermis that lacks osteonal structure.

An apical notch is absent from most adult nasal bosses, and the corresponding area of horn core instead forms a shallow transverse “step” across the rostral quarter of the nasal boss. In some individuals, a shallow longitudinal ridge runs across the dorsal surface of the nasal boss and continues as a more pronounced projection in the rostral step. Although this bony morphology differs from *Achelousaurus*, the osteological correlates superimposed on these larger-scale bony structures are identical, indicating similar skin structures.

The lateral surface of nasal bosses in *Pachyrhinosaurus canadensis* show a series of bony grooves and fins not unlike those seen on the supraorbital bosses of *Achelousaurus*. These structures indicate a thick cornified sheath growing at a low angle to the underlying bone surface; the orientation of the grooves reveals the direction of epidermal growth. The lateral grooves vary from a rostral slant in nasal bosses more similar to that of *Achelousaurus* to nearly vertical in the most derived examples (e.g., the Drumheller specimen of *Pachyrhinosaurus* cf. *P. canadensis*; Langston, 1967). Variation in the orientation of lateral grooves within the sample of *Pachyrhinosaurus lakustai* from Pipestone Creek suggests that the direction of growth for the cornified nasal pad was subject to ontogenetic or within-population variation.

The rostral comb (Currie et al., 2008; dorsal processes of the premaxillae and premaxillary processes of the nasals) shows a series of bony prominences not unlike those seen on the squamosals and parietals of centrosaurines in general. These prominences are interpreted as apophyseally ossified osteological correlates for epidermal scales, indicating a midline row of scales between the horny beak and the nasal boss. This differs from the single cornified sheath interpreted for *Centrosaurus*.

Skin correlates for the supraorbital region of adult *Pachyrhinosaurus lakustai* are variable, and similar to those seen both in adult *Einosaurus* and the holotype of *Achelousaurus*. Some individuals show a single pronounced apical pit with a basal sulcus (e.g., TMP 1989.55.21), indicating a cornified pad with a thinner cornified sheath about the edges. Other individuals show a relatively flattened boss with bony grooves and fins and no basal sulcus, indicating a cornified pad that did not trail out into a thin sheath. Both of these morphs occasionally show perforations in the boss that communicate with underlying parts of the frontal sinus system (Fig. 12D). Similar perforations can be seen on the bony frontal bosses of woodland muskoxen *Bootherium bombifrons* (e.g., USNM 2556) that communicate with the

paranasal sinuses. These perforations would be well-protected from injury in life by a thick pad of heavily cornified epidermis (Guthrie, 1992).

The supraorbital boss forms from the second in a sequence of three scales over the dorsal rim of the orbit, as indicated by shallow bony prominences rostral and caudal to the supraorbital boss itself. Two additional bony prominences on the squamosal indicate the continuation of the supraorbital scale row. Thus the epidermal scales over the orbit in *Pachyrhinosaurus* species are larger and less numerous than those seen in *Centrosaurus*.

A row of bony prominences on the parietal bar is interpreted as a series of scales similar to those of *Centrosaurus*, and in some individuals of *Pachyrhinosaurus lakustai*, one to three of these scales were elaborated into short horn sheaths, supported by bony horn cores (Fig. 12G). Similar elaboration of epidermal scales into projecting horns can be seen in extant *Phrynosoma* species. In at least one *Pachyrhinosaurus lakustai* individual (TMP 1987.55.81), the apex of the novel parietal horn core shows the pitted osteological correlate for a cornified pad, similar to the apical resorption seen on the horn cores of other centrosaurines.

Extant Analogs for Rugose Bosses in *Pachyrhinosaurus*: Results and Discussion

Convergence of structure and function in extant taxa. The thick cornified pads inferred to cover the rugose nasal and supraorbital bosses of *Pachyrhinosaurus* species were most similar to the cornified pads on the frontal bosses of adult male muskoxen, as the bony correlate seen in both taxa relates directly to the presence of papillary epidermis growing at comparatively steep angles to the bone surface. Muskoxen are the only extant species that show this particular relationship of strongly papillary epidermis and a bony boss. However, as a single species, muskoxen provide only a single data point for the relationship between this morphology and any putative related function. We have thus broadened our interpretation of "similar" skin structures in extant taxa to include any thickened cornified pad of epidermis that is not directly incorporated into a horn sheath, which includes adult male African buffalo *Synceurus*, adult male banteng *Bos javanicus*, and, among extant theropods, helmeted hornbills *Buceros vigil*.

In three of these four extant examples (*Ovibos*, *Synceurus*, and *Buceros vigil*), the presence of a thickened cornified pad has been noted to co-occur with headbutting behaviors that are more pronounced than those seen in sister taxa (Nowak and Paradiso, 1983; Lent, 1988; Kemp, 1995; Kinniard et al., 2003). No conclusive behavioral data for banteng have been published, leaving this taxon as an unknown as far as this potential structure/function relationship is concerned. The small sample of extant taxa with cornified pads, and their broad phylogenetic distribution (essentially encompassing Amniota), renders phylogenetic tests of character correlation impractical. Interdependence between a morphological character with two states (cornified sheath, cornified pad) and a behavioral character with two states (light clashing, headbutting) was examined in a sample of thirty extant taxa (Table 8), comprising the three poten-

tially analogous taxa and several of their close outgroup taxa. Skin morphology was scored using a combination of data from this study and published descriptions; behavior was scored using published accounts (citations listed in Table 8). The strength of any relationship between skin morphology and behavior was assessed using both Likelihood χ^2 with Williams' correction and Fisher's exact test in JMP 7. Skin morphology and agonistic behavior are strongly related (Table 9), with probabilities of independence that vary by test between $P = 0.0542$ (Fisher's exact test) and $P = 0.0239$ (Likelihood χ^2). Within this sample of species, the possession of a cornified pad can be seen as strongly related to the associated headbutting behavior. The relationship between cornified pads and headbutting in potentially analogous extant taxa (*Ovibos moschatus*, *Synceurus caffer*, and *Buceros vigil*) thus passes the first of the three tests of hypotheses of analogy (convergence) noted in the previous section.

Lundrigan (1996) discussed a functional relationship between robust, ventrally curving horns and headbutting in Bovidae, and thus the possession in *Ovibos* and *Synceurus* of a cornified epidermal pad on the dorsal side of a ventrally curved horn sheath can be seen as an extreme case of this more general phenomenon. When the taxa considered are scored instead for ventrally curved horn sheaths vs. other horn curvatures, the relationship between this character and headbutting is even more robust ($P = 0.0002$ by Likelihood χ^2 , $P = 0.0004$ by Fisher's exact test; Table 10), in line with the relationship between downward-pointing horn tips and ramming found by Caro et al. (2003). The ventrally curved nasal horn of *Einosaurus* is superficially similar to the ventrally curved horn of caprine bovids, but shows a pronounced mediolateral compression. This may have had the effect of increasing the second moment of area of the horn core in a dorsoventral axis, increasing its resistance to dorsoventral bending, but the mediolaterally narrow crown of the horn core is not similar to the relatively broad crowns of caprine horns. Thus the more general relationship between ventrally curving horns such as those seen in bighorn sheep (*Ovis canadensis*) and headbutting behavior conditionally passes the test of convergence as a potential analog for the ventrally curving nasal horn of *Einosaurus*. A closer examination of the mechanical consequences of loading *Einosaurus* nasal horn cores, or an exploratory analysis of possible points of contact for the nasal and supraorbital horn cores (after Farke, 2004) may resolve some of the ambiguity associated with the similarity between this horn shape and the ventrally curved horns of caprine bovids.

Tests of adaptation in extant taxa. Ancestral character state reconstructions of the three characters discussed (cornified pad, robust ventrally curved horns, and headbutting) match an expected pattern for adaptation in all three potentially analogous clades (Caprinae, Bovinae, and Bucerotidae), but the match for adaptive pattern is more robust in Bucerotidae and Caprinae than it is in Bovinae.

The pattern of character state evolution in hornbills (Bucerotidae) is straightforward: helmeted hornbills (*Buceros vigil*) are the only bucerotid taxon that exhibits

TABLE 8. Extant taxa with cornified pads and sister taxa used to assess relationship between skin morphology and agonistic behavior

Taxon	Cornified skin morphology	Agonistic behavior	Horn shape	Reference
<i>Naemorhedus goral</i> ^a	Sheath	Light clashing	Straight	Mead, 1989
<i>Ovibos moschatus</i> ^a	Pad	Headbutting	Ventrally curved	Lent, 1988
<i>Oreamnos americanus</i> ^a	Sheath	Light clashing	Straight	Rideout and Hoffman, 1975
<i>Ovis dalli</i> ^a	Sheath	Headbutting	Ventrally curved	Bowyer and Leslie, 1992
<i>Ovis ammon</i> ^a	Sheath	Headbutting	Ventrally curved	Fedosenko and Blank, 2005
<i>Ammotragus lervia</i> ^a	Sheath	Headbutting	Ventrally curved	Gray and Simpson, 1980
<i>Capricornis crispus</i> ^a	Sheath	Headbutting	Straight	Jass and Mead, 2004
<i>Pseudois nayaur</i> ^a	Sheath	Headbutting	Ventrally curved	Wang and Hoffman, 1987
<i>Capra cylindricornis</i> ^a	Sheath	Headbutting	Ventrally curved	Weinberg, 2002
<i>Capra sibirica</i> ^a	Sheath	Headbutting	Ventrally curved	Fedosenko and Blank, 2001
<i>Budorcas taxicolor</i> ^a	Sheath	Light clashing	Ventrally curved	Neas and Hoffman, 1987
<i>Ovis canadensis</i> ^a	Sheath	Headbutting	Ventrally curved	Shackleton, 1985
<i>Anthracoceros albirostris</i> ^b	Sheath	Light clashing	Straight	Kemp, 1995
<i>Anthracoceros malayanus</i> ^b	Sheath	Light clashing	Straight	Kemp, 1995
<i>Buceros bicornis</i> ^b	Sheath	Light clashing	Straight	Kemp, 1995
<i>Buceros vigil</i> ^b	Pad	Headbutting	Straight	Kemp, 1995
<i>Aceros corrugatus</i> ^b	Sheath	Light clashing	Straight	Kemp, 1995
<i>Penelopides panini</i> ^b	Sheath	Light clashing	Straight	Kemp, 1995
<i>Buceros hydrocorax</i> ^b	Sheath	Light clashing	Straight	Kemp, 1995
<i>Buceros rhinoceros</i> ^b	Sheath	Light clashing	Straight	Kemp, 1995
<i>Anthracoceros montani</i> ^b	Sheath	Light clashing	Straight	Kemp, 1995
<i>Anthracoceros marchei</i> ^b	Sheath	Light clashing	Straight	Kemp, 1995
<i>Anthracoceros coronatus</i> ^b	Sheath	Light clashing	Straight	Kemp, 1995
<i>Bison bison</i> ^c	Sheath	Headbutting	Straight	Meagher, 1986
<i>Taurotragus oryx</i> ^c	Sheath	Light clashing	Straight	Pappas, 2002
<i>Syncerus caffer</i> ^c	Pad	Headbutting	Ventrally curved	Nowak and Paradiso, 1983
<i>Tragelaphus angasii</i> ^c	Sheath	Light clashing	Straight	Nowak and Paradiso, 1983
<i>Tragelaphus scriptus</i> ^c	Sheath	Light clashing	Straight	Nowak and Paradiso, 1983
<i>Tragelaphus strepsiceros</i> ^c	Sheath	Light clashing	Straight	Nowak and Paradiso, 1983
<i>Boselaphus tragocamelus</i> ^c	Sheath	Light clashing	Straight	Nowak and Paradiso, 1983

^aCaprinae.^bBucerotidae.^cBovinae.**TABLE 9. Contingency table test results for agonistic behavior × cornified sheath morphology**

<i>N</i>	DF	–Log-Likel	<i>R</i> ²
30	1	3.005	0.1488
Test	<i>X</i> ²	<i>P</i>	
Likelihood ratio	6.009	0.0142*	
With Williams' correction	5.100	0.0239*	
Fisher's exact test	–	0.0542	

–Log-Likel: negative log-likelihood.

Williams' correction applied to the Likelihood χ^2 to correct for small sample size.*Statistically significant at *P* = 0.05.**TABLE 10. Contingency table test results for agonistic behavior × horn shape**

<i>N</i>	DF	–Log-Likel	<i>R</i> ²
30	1	8.485	0.4203
Test	<i>X</i> ²	<i>P</i>	
Likelihood ratio	16.971	<0.0001*	
With Williams' correction	13.732	0.0002*	
Fisher's exact test	–	0.0004*	

–Log-Likel: negative log-likelihood.

Williams' correction applied to the Likelihood χ^2 to correct for small sample size.*Statistically significant at *P* = 0.05.

either of the derived traits of a cornified epidermal pad or headbutting, leading to unequivocal reconstruction of both traits on the same branch in all trees used for this test (Fig. 13). Although other functions have been suggested for the pad of “hornbill ivory” seen in this taxon (Cats-Kuenen, 1961), headbutting is the only function that does not also occur in sister taxa (Kemp, 1995; Cranbrook and Kemp, 1995; Kinniard et al., 2003). The cornified pad of *Buceros vigil* thus passes the second of the three tests of analogy (aptation).

The pattern of character state evolution in cattle (Bovinae) is clouded by a lack of detailed behavioral data for many bovine taxa, and as such does not provide

a solid basis for inferring function in extinct taxa. Ancestral character states based on the available information are shown in Fig. 14, using the published topology and branch lengths of Fernández and Vrba (2005). The topology of Hassanin and Ropiquet (2004) was also used for this test, with similar results. A majority of reconstructions (six of ten: MP, ML with Grafen branch lengths, and ML with branch lengths of one for both topologies) place headbutting as a primitive character state for Bovini. The most conservative picture that emerges from ancestral character state reconstruction in this system is that the putative selection regime (headbutting) appeared 5–15 Ma before the morphological change

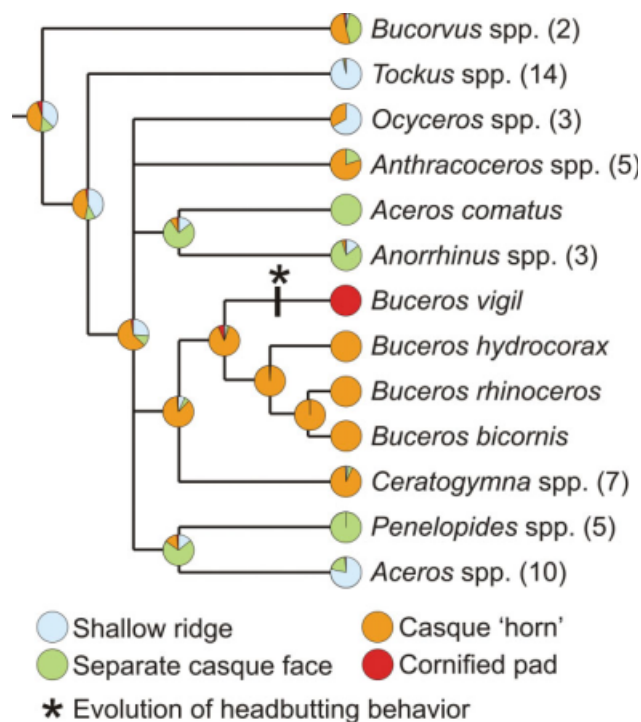


Fig. 13. Ancestral character state reconstructions of casque morphology and headbutting behavior in Bucerotidae (hornbills). A casque with a projecting "horn" is unequivocally reconstructed for *Ceratogymna*+*Buceros*, and the transition to a cornified pad in *Buceros vigil* is accompanied by a transition from light bill clashing to headbutting behaviors (asterisk). Nodes show proportional likelihoods for each morphological character state with Pagel (1992) transformed branch lengths. Topology after Kemp (1995).

(cornified pad). This pattern is still in line with that expected for adaptation (Baum and Larson, 1991; Fig. 5B), but the inferred time lag between selection regime and adaptation increases the chance that the co-occurrence of these two traits is a false positive. The cornified pad of adult male *Syncerus* thus conditionally fails the aptation test for analogy, and will not be considered as an appropriate analogous system for assessing function in *Pachyrhinosaurus*.

In contrast, the pattern of character state change in sheep and goats (Caprinae) provides a more compelling case for the relationship between horn shape and headbutting behavior. When the transition to a cornified pad is reconstructed alongside the transition to headbutting, MP and ML analyses of both of the phylogenies used in this study [Fig. 15; topologies of Ropiquet and Hassanin (2005) and Lalueza-Fox et al. (2005)] all place one of three or four unequivocal transitions to headbutting on the branch leading to *Ovibos*, the same branch as the transition to a cornified pad. When horn morphology is scored for either robust, ventrally curving horns or other horn shapes (as shown previously for the character correlation test), ML analyses match all of the transitions to headbutting with a transition to robust, ventrally curving horns on the same branch (Fig. 15). Cornified pads in *Ovibos* thus pass the aptation test of analogy.

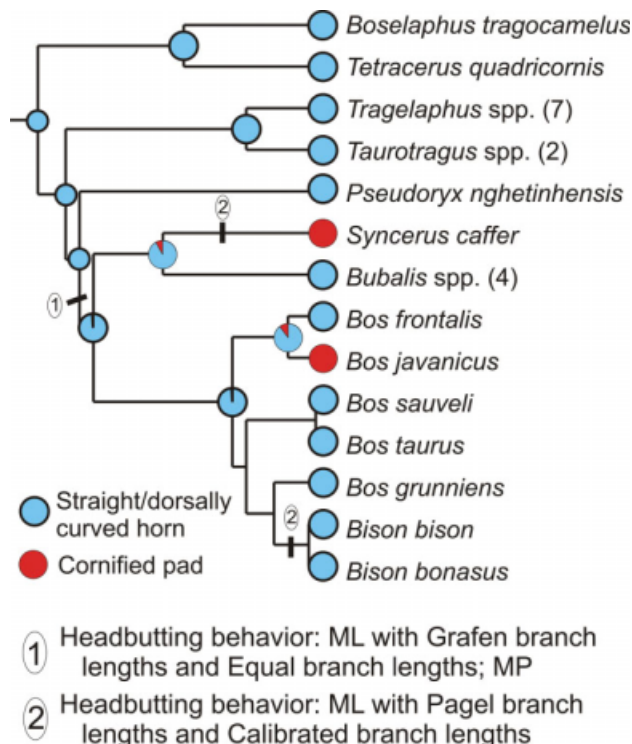


Fig. 14. Ancestral character state reconstructions of horn morphology and headbutting behavior in Bovinae (cattle and allies). Nodes show proportional likelihoods for each morphological character state with the published topology and branch lengths of Fernández and Vrba (2005).

Similarity in transformation sequences among extant analogs and centrosaurines. The transition from straight horn core to robust ventrally curved horn-core and flattened boss in Centrosaurinae (Fig. 16) is similar to several morphological transitions seen within Caprinae. The strongest similarity occurs between the pattern of centrosaurine horn evolution and the transition from primitive straight horn cores such as those seen in goral (*Naemorhedus*) and serow (*Capricornis*) to a rugose boss in muskoxen (*Ovibos*). These examples pass the third test of analogy (correspondence) and stand as the most appropriate extant analogs for assessing the function of rugose bosses in *Achelousaurus* and *Pachyrhinosaurus*.

The morphological transition seen in Bucerotidae shows a transition from a slightly different starting point (a thin-walled projecting casque, e.g., *Buceros hydrocorax*) to a similar endpoint (the thick cornified casque of *Buceros vigil*). This transition is conditionally accepted in our correspondence test for analogy. The cornified pad of *Buceros vigil* thus provides an appropriate analog for assessing the function of rugose bosses in *Pachyrhinosaurus* and *Achelousaurus*, but carries less weight in this assessment than the cornified pad of muskoxen.

Function of rugose bosses in centrosaurine dinosaurs. Both of the extant analogous systems for the rugose bosses of centrosaurine dinosaurs consist of thick pads of cornified epidermis that function as contact

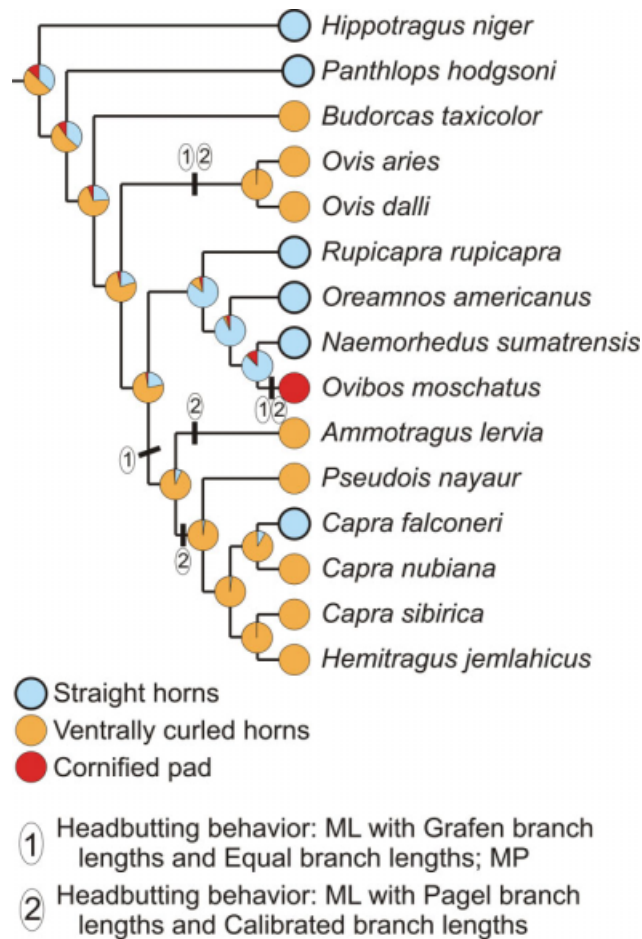


Fig. 15. Ancestral character state reconstructions of horn morphology and headbutting behavior in Caprinae (goats and sheep) and outgroups. Nodes show proportional likelihoods for each morphological character state with Pagel (1992) transformed branch lengths and the topology of Ropiquet and Hassanin (2005).

surfaces for butting or ramming. Butting or ramming with the head (either to an opponent's head or to another area, such as the flank) is thus the most likely hypothesis of function for the rugose bosses in centrosaurine dinosaurs, in a manner similar to that conceived for the nasal boss of *Pachyrhinosaurus* by Sternberg (1950) and Farlow and Dodson (1975). The change in horn morphology over time within Centrosaurinae is thus consistent with a linear trend of increasing intensity in agonistic behaviors, starting with horn clashing in basal centrosaurines with longer supraorbital horns (Farke, 2004; Farke et al., 2009) and ending in high-energy headbutting.

DISCUSSION

Summary of centrosaurine facial skin morphology

Centrosaurine dinosaurs show a diverse array of bony facial morphologies but a comparatively narrow range of osteological correlates for skin structures. Most bony morphology on centrosaurine skulls that can be attrib-

uted to skin structures indicates a progression from shallow epidermal scales (generally in the range of 5–10 cm in diameter in adult skulls), to tall cornified horn sheaths, to thick pads of cornified epidermis that initially develop at the apices of horn sheaths, ending in massive cornified pads across the skull roof (Fig. 16). This progression can be seen at different stages in different skull regions. For example, the progression from scales to taller horn sheaths can be seen in the development of the parietal bar scales of basal centrosaurines into short horns in *Pachyrhinosaurus lakustai* (Fig. 12G), whereas the progression of taller horn sheaths into massive cornified pads can be seen in the transition between the nasal horn sheath of basal centrosaurines and the nasal pad of *Achelousaurus* (Fig. 16). Pronounced scales and short horns are both present on *Pachyrhinosaurus canadensis*, but the majority of the skull roof is occupied by massive cornified pads on the nasal and supraorbital bosses (Fig. 12A).

Our reconstruction of thick cornified pads on the nasal and supraorbital bosses of *Pachyrhinosaurus* is not only derived from histological and morphological similarities to the horns of living muskoxen, but also from the ways in which *Pachyrhinosaurus* differs from the morphology and histology predicted for other hypotheses of skin shape. The tall, rhinoceros-like epidermal horns that constitute the other major competing hypothesis for *Pachyrhinosaurus* horn shape provide a specific set of morphological and histological predictions: (1) the periphery of both nasal and supraorbital bosses should show a bone surface texture (projecting rugosity) that is distinct from the bone surface texture on the center of the bosses (smooth bone with normal neurovascular foramina), and (2) the projecting rugosity on the boss should be formed entirely of metaplastically ossified dermal collagen fibers. The morphology and histology of the rugose bosses of centrosaurine dinosaurs do not meet either of these predictions. The similarity between the bosses of *Pachyrhinosaurus* and the horn attachments of living rhinoceros is thus only superficial.

Patterns of ossification in centrosaurine ornaments

Some of the scale-related elements on ceratopsian skulls are clearly separate ossification centers (e.g., epinasal and episquamosal ossifications; Hatcher et al., 1907; Horner and Goodwin, 2008), while others appear to be direct outgrowths of the dermatocranium (e.g., parietal eminences). The presence of both types of scale correlate on ceratopsian skulls agrees with the pattern found in Ankylosauria by Vickaryous et al. (2001). Unlike extant squamates, for which osteoderms and apophyseal scale correlates are largely confined to separate clades, ornithischian dinosaurs had both forms of scale-related bone growth. Thus, while we might expect to find either osteoderms or apophyseal eminences forming ornaments in ornithischian dinosaurs, the critical point is that both of these features can be directly related to homologous unpreserved skin features.

The similarity between osteoderms and apophyseally demarcated scale correlates opens up several new possibilities for comparing inferred skin structures across ornithischian groups. For example, despite the fact that the bony elements that compose the nasal horn core in

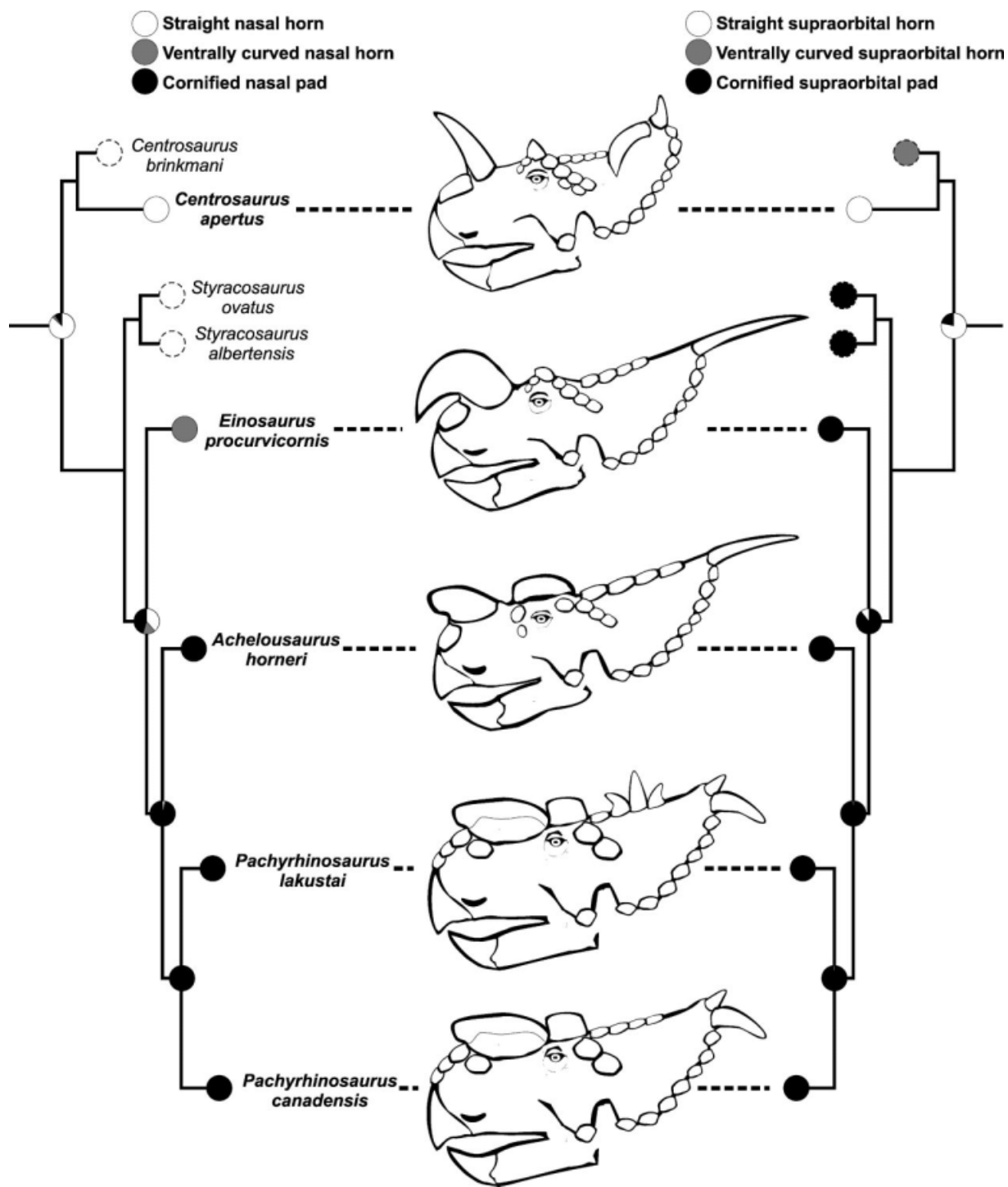


Fig. 16. ML Ancestral character state reconstructions of nasal and supraorbital horn morphology in centrosaurine dinosaurs. The transition from straight horns in basal centrosaurines to ventrally curved nasal horns and cornified pads in derived centrosaurines is similar to the morphological transitions associated with headbutting behavior in extant caprines. The primitive polymorphism of supraorbital horn cores in *Centrosaurus* (Sampson et al., 1997) is canalized in more derived

centrosaurines, and this development is followed by the progression of ventrally curved nasal horns and cornified pads in *Einiosaurus*, *Achelousaurus*, and *Pachyrhinosaurus*. Character states for *Centrosaurus brinkmani*, *Styracosaurus ovatus*, and *Styracosaurus albertensis* were taken from published descriptions, and were not included in ancestral character state reconstructions.

centrosaurine and chasmosaurine ceratopsians are non-homologous, the skin structures that induce the growth of the horn core may themselves be homologous, deriving from a single scale in a common ancestor. The Wahweap centrosaurine (Kirkland and Deblieux, 2007) may provide more information to test this hypothesis of homology.

The supraorbital horn cores of some chasmosaurine ceratopsians, including *Chasmosaurus belli*, *C. irvinensis*, and *C. russelli*, are sometimes preserved as shallow rugose pits, in a manner very similar to that seen for derived centrosaurines (Dodson et al., 2004). The horn sheath covering the supraorbital horn core is likely to be homologous between centrosaurines and chasmosaurines. The similarity in bone surface features between pitted chasmosaurine and centrosaurine supraorbital horn cores may very well be due to similar processes in horn sheath growth, i.e., the transition from a thin horn sheath to a thick cornified pad.

The supraorbital, postorbital, and squamosal nodes seen on pachycephalosaurian dinosaurs (Maryańska et al., 2004) indicate a pattern of pronounced scales similar to that inferred on the same skull elements of centrosaurine dinosaurs in this study. As noted by Vickaryous et al. (2001) for ankylosaurs, the scale patterns visible on ceratopsians and pachycephalosaurs are strikingly similar in some respects to those seen in extant squamates. Further comparisons of scale correlates in ornithischians may shed more light the cause of this similarity.

Species recognition, sexual selection, and social selection in Centrosaurinae

The bony ornaments of ceratopsian dinosaurs have been suggested to function predominantly in intraspecific communication, but there is ongoing debate as to whether this communication only served the purpose of species recognition or if it was involved in intraspecific sexual selection as well (Farlow and Dodson, 1975; Spassov, 1979; Sampson et al., 1997; Padian et al., 2004; Goodwin et al., 2006). Morphological evolution driven by species recognition is expected to show a different pattern of character state change than morphological evolution driven by sexual selection (Padian et al., 2004): (1) Species recognition is expected to occur where the ranges of several closely related species overlap, whereas sexual selection may occur both in sympatry and in isolation. (2) Species recognition is expected to result in nonlinear, diverging trends of morphological evolution, whereas sexual selection is expected to result in linear trends. And finally, (3) differences in parental investment between males and females are expected to cause dimorphism in sexually selected characters (Darwin, 1871; Emlen and Oring, 1977), but no similar tendency to dimorphism has been suggested for species recognition. Sympatry and nonlinear trends of divergence both occur frequently in nonavian dinosaur clades (Padian et al., 2004), fitting the pattern expected for species recognition. Clear-cut sexual dimorphism in nonavian dinosaurs has been elusive, leading to the current assessment of bony ornaments such those of *Pachyrhinosaurus* as the result of species recognition, not sexual selection (Padian et al., 2004; Goodwin et al., 2006).

Based on the headbutting function inferred for the rugose bosses of *Pachyrhinosaurus*, we suggest that the concept of “social selection” (West-Eberhard, 1983) offers

a more compatible form of selection to drive the diversity seen in centrosaurine cranial ornaments. Social selection occurs when there is differential success in within-species competition for any limited resource. The limited resource may be mating opportunities, resulting in sexual selection as a subcategory of social selection, or the limited resource may be a feeding or breeding territory, equally contested and defended by either sex. Some predictions of social selection are similar to those of species recognition (Payne, 1983; West-Eberhard, 1983), but there are differences that allow the predictions to be tested in fossil taxa such as ceratopsians. Two differences stand out: (1) socially selected traits can function in any phase of courtship or in social interactions outside of mating, whereas species recognition traits are under selection only in the earliest stages of courtship during mating; and (2) socially selected traits may persist and diverge in allopatric isolated populations, whereas species recognition traits are only expected to occur in closely related sympatric species (West-Eberhard, 1983, p 166–167).

The headbutting behavior inferred for derived centrosaurines here (and inferred for derived chasmosaurines by other authors; viz. Farke et al., 2009) would have been comparatively expensive and risky. In the extant caprines that show similar behaviors, headbutting is a late occurrence in intraspecific aggression, generally occurring after a series of visual and auditory displays (Geist, 1966; Gray and Simpson, 1980; Lent, 1988; Weinberg, 2002; Fedosenko and Blank, 2005). In both caprines and helmeted hornbills, headbutting is a coordinated behavior in which both participants proceed through a series of stereotyped, ritualized behaviors before and after impact (Geist, 1966; Kinniard et al., 2003; Fedosenko and Blank 2005). The presence of displays and coordinating behaviors leading up to headbutting in extant taxa suggests that the morphological changes seen in derived centrosaurine horns for headbutting were driven by selection on behaviors that occurred well after early and relatively inexpensive opportunities for species recognition by visual cues. Although they may have been exapted to function in species recognition, the rugose bosses of *Achelousaurus* and *Pachyrhinosaurus* do not match the pattern expected for species recognition without social selection.

ACKNOWLEDGMENTS

The authors thank Brian Beatty, Audrone Biknevičius, Lisa Noelle Cooper, Joseph Daniel, David Dufeu, David Evans, Andrew Farke, Cynthia Marshall Faux, Mark Goodwin, Sue Herring, Robert Hill, Casey Holliday, Dominique Homberger, Angela Horner, Jack Horner, John Hutchinson, Andrew Lee, Eric McElroy, Hillary Maddin, Paul Maderson, Matt Milbachler, Donald Miles, Patrick O'Connor, Chris Organ, Kevin Padian, Erin Rasmusson, Steve Reilly, Michael Ryan, Natalia Rybczynski, Torsten Scheyer, Nancy Stevens, Alycia Stigall, Takanobu Tsuihiji, Matt Vickaryous, and Susan Williams who have all greatly aided this research. For access to histology and microscopy equipment the authors thank Dan Hembree, David Kidder, Greg Nadon, Patrick O'Connor, Gar Rothwell, and Susan Williams. For access to tissue specimens, the authors thank Casey Holliday; Evan Blumer, Mark Atkinson, and Steve Shurter at The Wilds; and Gretchen Bickert at the

Phoenix Zoo. David Dufeu and Ryan Ridgely at OU μ CT and Heather Mayle at O'Bleness Memorial Hospital provided invaluable assistance with CT scanning. For access to osteological and paleontological specimens, the authors thank James Gardner at the Royal Tyrrell Museum; Jack Horner, Pat Lieggi, Carrie Ancell, Bob Harmon, David Varrichio, Ellen-Thérèse Lamm, and Susan Winking at the Museum of the Rockies; Kevin Seymour and Mark Peck at the Royal Ontario Museum; Greg Schneider and Janet Hinshaw at the University of Michigan Museum of Zoology; Mark Goodwin, Pat Holroyd, and Kevin Padian at the University of California Museum of Paleontology; Steve Rogers and Suzanne McLaren at the Carnegie Museum of Natural History; Linda Gordon, Robert Purdy, and Matt Carrano at the National Museum of Natural History; Eileen Westwig, Paul Sweet, Susan Bell, Carl Mehling, and Mark Norell at the American Museum of Natural History; Christine Lefèvre and Alexis Martin at the Muséum national d'Histoire naturelle; Gerald Mayer at the Naturmuseum Senckenberg; Link Olson at the University of Alaska Museum; and Scott Sampson, Mike Getty, Mark Loewen, and Eric Lund at the University of Utah Museum of Paleontology.

LITERATURE CITED

- Baum DA, Larson A. 1991. Adaptation reviewed: a phylogenetic methodology for studying character macroevolution. *Syst Zool* 40:1–18.
- Berger J, Cunningham C. 1998. Natural variation in horn size and social dominance and their importance to the conservation of black rhinoceros. *Conserv Biol* 12:708–711.
- Bowyer RT, Leslie DM. 1992. *Ovis dalli*. *Mamm Species* 393:1–7.
- Breiman L, Friedman JH, Olshen RA, Stone CJ. 1984. Classification and regression trees. New York: Chapman and Hall.
- Brown B, Schlaikjer EM. 1940. The origin of ceratopsian horn-cores. *Am Mus Novit* 1065:1–7.
- Caro TM, Graham CM, Stoner CJ, Flores MM. 2003. Correlates of horn and antler shape in bovids and cervids. *Behav Ecol Sociobiol* 55:32–41.
- Bustard HR. 1958. Use of horns by *Chamaeleo jacksoni*. *Brit J Herpetol* 2:105–107.
- Cats-Kuenen CSWM. 1961. Casque and bill of *Rhinoplax vigil* (Forst.) in connection with the architecture of the skull. *Verhandelingen der Koninklijke Nederlandsche Academie van Wetenschappen., Afdeling Natuurkunde* 53:1–51.
- Coddington JA. 1988. Cladistic tests of adaptational hypotheses. *Cladistics* 4:3–22.
- Coddington JA. 1990. Bridges between evolutionary pattern and process. *Cladistics* 6:379–386.
- Cranbrook E, Kemp AC. 1995. Aerial casque-butting by hornbills (Bucerotidae): a correction and an expansion. *Ibis* 137:588–589.
- Currie PJ. 1989. Long-distance dinosaurs. *Nat Hist* 6:60–65.
- Currie PJ, Langston W, Jr., Tanke DH. 2008. A new species of *Pachyrhinosaurus* (Dinosauria, Ceratopsidae) from the Upper Cretaceous of Alberta, Canada. In: Currie PJ, Langston W, Jr., Tanke DH, editors. A new horned dinosaur from an Upper Cretaceous Bone Bed in Alberta. Ottawa: NRC Research Press. p 1–108.
- Darwin C. 1871. The descent of man, and selection in relation to sex. London: John Murray.
- Dinerstein E. 1991. Sexual dimorphism in the greater one-horned rhinoceros (*Rhinoceros unicornis*). *J Mammal* 72:450–457.
- Dodson P, Forster CA, Sampson SD. 2004. Ceratopsidae. In: Weishampel DB, Dodson P, Osmólska H, editors. The Dinosauria. Berkeley: University of California Press. p 494–513.
- Edwards SJ, Russell AP. 1994. Bone tissue patterns and the growth of the nasal complex in the horned dinosaur *Pachyrhinosaurus*. *Bull Can Soc Zool* 25:47–48.
- Eibl-Eibesfeldt I. 1966. The fighting behaviour of marine iguanas. *Philos Trans R Soc Ser B Biol Sci* 251:475–476.
- Emlen ST, Oring LW. 1977. Ecology, sexual selection, and the evolution of mating systems. *Science* 197:215–223.
- Farke AA. 2004. Horn use in *Triceratops* (Dinosauria: Ceratopsidae): testing behavioral hypotheses using scale models. *Palaeontol Electron* 7:10.
- Farke AA, Wolff EDS, Tanke DH. 2009. Evidence of combat in *Triceratops*. *PLoS ONE* 4:e4252.
- Farlow JO, Dodson P. 1975. The behavioral significance of frill and horn morphology in ceratopsian dinosaurs. *Evolution* 29:353–361.
- Fedosenko AK, Blank DA. 2001. *Capra sibirica*. *Mamm Species* 675:1–13.
- Fedosenko AK, Blank DA. 2005. *Ovis ammon*. *Mamm Species* 773:1–15.
- Feldesman MR. 2002. Classification trees as alternatives to linear discriminant analysis. *Am J Phys Anthropol* 119:257–275.
- Fernández MH, Vrba ES. 2005. A complete estimate of the phylogenetic relationships in Ruminantia: a dated species-level supertree of the extant ruminants. *Biol Rev* 80:269–302.
- Francillon-Vieillot H, de Buffrénil V, Castanet J, Géraudie J, Meunier FJ, Sire JY, Zylberberg L, de Ricqlès A. 1990. Microstructure and mineralization of vertebrate skeletal tissues. In: Carter JG, editor. Skeletal Biomineralization: Patterns, Processes and Evolutionary Trends, vol. 1. New York: Van Nostrand Reinhold. p 471–530.
- Geist V. 1966. The evolution of horn-like organs. *Behaviour* 27:175–214.
- Goodwin MB, Clemens WA, Horner JR, Padian K. 2006. The smallest known *Triceratops* skull: new observations on ceratopsid cranial anatomy and ontogeny. *J Vert Paleontol* 26:103–112.
- Gould SJ, Lewontin RC. 1979. The spandrels of San Marco and the Panglossian paradigm: a critique of the adaptationist programme. *Proc R Soc Lond Ser B Biol Sci* 205:581–598.
- Gould SJ, Vrba ES. 1982. Exaptation; a missing term in the science of form. *Paleobiology* 8:4–15.
- Grafen A. 1989. The phylogenetic regression. *Philos Trans R Soc Lond Ser B Biol Sci* 326:119–157.
- Grandcolas P, d'Haese C. 2003. Testing adaptation with phylogeny: how to account for phylogenetic pattern and selective value together. *Zool Ser* 32:483–490.
- Gray GG, Simpson CD. 1980. *Ammotragus lervia*. *Mamm Species* 144:1–7.
- Greene HW. 1986. Diet and arboreality in the emerald monitor, *Varanus prasinus*, with comments on the study of adaptation. *Fieldiana Zool* 31:1–12.
- Guthrie RD. 1992. New paleoecological and paleoethological information on the extinct helmeted muskoxen from Alaska. *Annal Zool Fennici* 28:175–186.
- Hassanin A, Ropiquet A. 2004. Molecular phylogeny of the tribe Bovini (Bovidae, Bovinae) and the taxonomic status of the Kouprey, *Bos sauveli* Urbain 1937. *Mol Phylogenet Evol* 33:896–907.
- Hatcher JB, Marsh OC, Lull RS. 1907. The Ceratopsia. *US Geol Surv Monogr* 49:1–300.
- Hieronymus TL, Witmer LM. Adaptation, exaptation, and convergence in rhinocerotid horn evolution *Proc R Soc B Biol Sci* Submitted for publication.
- Homberger DG. 2001. The case of the cockatoo bill, horse hoof, rhinoceros horn, whale baleen, and turkey beard: the integument as a model system to explore the concepts of homology and non-homology. In: Dutta HM, Datta Munshi JS, editors. Vertebrate functional morphology: horizon of research in the 21st century. Enfield: Science Publishers. p 317–343.
- Horner JR, Goodwin MB. 2006. Major cranial changes during *Triceratops* ontogeny. *Proc R Soc B Biol Sci* 273:2757–2761.
- Horner JR, Goodwin MB. 2008. Ontogeny of cranial epi-ossifications in *Triceratops*. *J Vert Paleontol* 28:134–144.
- Horner JR, Marshall C. 2002. Keratinous covered dinosaur skulls. *J Vert Paleontol* 22:67A.
- Jass CN, Mead JI. 2004. *Capricornis crispus*. *Mamm Species* 750:1–10.

- Kaiser HE. 1960. Untersuchungen zur vergleichenden Osteologie der fossilen und rezenten Pachyostosen. *Palaeontograph Abteilung A* 114:113–196.
- Kemp AC. 1995. *The hornbills: bucerotiformes*. Oxford: Oxford University Press.
- Kinniard MF, Hadiprakarsa Y-Y, Thiensongrusamee P. 2003. Aerial jousting by helmeted hornbills *Rhinoplax vigil*: Observations from Indonesia and Thailand. *Ibis* 145:506–508.
- Kirkland J, DeBlieux D. 2007. New basal centrosaurine ceratopsian skulls from the Wahweap Formation (Middle Campanian), Grand Staircase—Escalante National Monument, Southern Utah. In: Ryan MJ, Chinnery-Allgeier BJ, Eberth DA, editors. *New perspectives on horned dinosaurs*. Bloomington: Indiana University Press.
- Kluge AG. 2005. Testing lineage and comparative methods for inferring adaptation. *Zool Scr* 34:653–663.
- Lalueza-Fox C, Castresana J, Sampietro L, Marques-Bonet T, Alcover JA, Bertranpetit J. 2005. Molecular dating of caprines using ancient DNA sequences of *Myotragus balearicus*, an extinct endemic Balearic mammal. *BMC Evol Biol* 5:70.
- Landmann L. 1986. The skin of reptiles: epidermis and dermis. In: Bereiter-Hahn J, Matoltsy AG, Richards KS, editors. *Biology of the integument. Vertebrates*. In: Bolk L, Goppert E, Kallius E, Lubosch W, editors. *Handbuch der Vergleichenden Anatomie der Wirbeltiere*. Berlin: Urban und Schwarzenberg. p 375–448.
- Langston W, Jr. 1967. The thick-headed ceratopsian dinosaur *Pachyrhinosaurus* (Reptilia: Ornithischia), from the Edmonton Formation near Drumheller, Canada. *Can J Earth Sci* 4:171–186.
- Langston W, Jr. 1975. The ceratopsian dinosaurs and associated lower vertebrates from the St. Mary River Formation (Maastrichtian) at Scabby Butte, southern Alberta. *Can J Earth Sci* 12:1576–1608.
- Larson A, Losos JB. 1996. Phylogenetic systematic of adaptation. In: Rose MR, Lauder GV, editors. *Adaptation*. San Diego: Academic Press. p 187–220.
- Lent PC. 1988. *Ovibos moschatus*. *Mamm Species* 302:1–9.
- Lundrigan B. 1996. Morphology of horns and fighting behavior in the family Bovidae. *J Mammal* 77:462–475.
- Maddison WP, Maddison DR. 2006. *StochChar*: a package of mesquite modules for stochastic models of character evolution. v1.1. Available at: <http://mesquiteproject.org>.
- Maddison WP, Maddison DR. 2008. *Mesquite*: a modular system for evolutionary analysis. v2.5. Available at: <http://www.mesquiteproject.org>.
- Marsh OC. 1887. Notice of some new fossil mammals. *Am J Sci* 34:323–331.
- Maryańska T, Chapman RE, Weishampel DB. 2004. *Pachycephalosauria*. In: Weishampel DB, Dodson P, Osmólska H, editors. *The Dinosauria*, 2nd ed. Berkeley: University of California Press. p 464–477.
- Mead JI. 1989. *Nemorhaedus goral*. *Mamm Species* 335:1–5.
- Meagher M. 1986. *Bison bison*. *Mamm Species* 266:1–8.
- Molnar RE. 1977. Analogies in the evolution of combat and display structures in ornithopods and ungulates. *Evol Theory* 3:165–190.
- Neas JF, Hoffman RS. 1987. *Budorcas taxicolor*. *Mamm Species* 277:1–7.
- Nowak RM, Paradiso JL. 1983. *Walker's mammals of the World*, 4th ed. Baltimore: Johns Hopkins University Press.
- Padian K, Horner JR, Dhalwal J. 2004. Species recognition as the principal cause of bizarre structures in dinosaurs. *J Vert Paleontol* 24:100A.
- Pagel M. 1992. A method for the analysis of comparative data. *J Theor Biol* 156:431–442.
- Pagel M. 1994. Detecting correlated evolution on phylogenies: A general method for the comparative analysis of discrete characters. *Proc R Soc Lond Ser B Biol Sci* 255:37–45.
- Pagel M, Meade A. 2006. Bayesian analysis of correlated evolution of discrete characters by reversible-jump Markov chain Monte Carlo. *Am Nat* 167:808–825.
- Pappas LA. 2002. *Taurotragus oryx*. *Mamm Species* 689:1–5.
- Payne RB. 1983. Bird songs, sexual selection, and female mating strategies. In: Waser S, editor. *Social behavior of female vertebrates*. New York: Academic Press. p 55–90.
- Reznick D, Travis J. 1996. The empirical study of adaptation in natural populations. In: Rose MR, Lauder GV, editors. *Adaptation*. San Diego: Academic Press. p 243–289.
- Rideout CB, Hoffman RS. 1975. *Oreamnos americanus*. *Mamm Species* 63:1–6.
- Ropiquet A, Hassanin A. 2005. Molecular phylogeny of caprines (Bovidae, Antilopinae): the question of their origin and diversification during the Miocene. *J Zool System Evol Res* 43: 49–60.
- Ryan MJ, Eberth DA, Brinkman DB, Currie PJ, and Tanke DH. 2009. A new *Pachyrhinosaurus*-like ceratopsid from the upper Dinosaur park formation (Late Campanian) of Southern Alberta, Canada. In: Ryan MJ, Chinnery-Allgeier BJ, Eberth DA, editors. *New perspectives on horned dinosaurs*. Bloomington: Indiana University Press.
- Ryan MJ, Russell AP. 2005. A new centrosaurine ceratopsid from the Oldman Formation of Alberta and its implications for centrosaurine taxonomy and systematics. *Can J Earth Sci* 42:1369–1387.
- Sampson SD. 1995. Two horned dinosaurs from the Upper Cretaceous two medicine formation of Montana; with a phylogenetic analysis of the Centrosaurinae (Ornithischia: Ceratopsidae). *J Vert Paleontol* 15:743–760.
- Sampson SD, Ryan MJ, Tanke DH. 1997. Craniofacial ontogeny in centrosaurine dinosaurs (Ornithischia: Ceratopsidae): taxonomic and behavioral implications. *Zool J Linn Soc* 121:293–337.
- Sawyer RH, Knapp LW, O'Guin WM. 1986. The skin of birds: epidermis, dermis, and appendages. In: Bereiter-Hahn J, Matoltsy AG, Richards KS, editors. *Biology of the integument*. In: Rose MR, Lauder GV, editors. *Adaptation*. San Diego: Academic Press. p 149–185.
- Sober E. 1984. *The nature of selection*. Cambridge: MIT Press.
- Sokolov VE. 1982. *Mammal skin*. Berkeley: University of California Press.
- Spassov NB. 1979. Sexual selection and the evolution of horn-like structures of ceratopsian dinosaurs. *Paleontol Stratigraph Lithol* 11:37–48.
- Sterchi DL, Eurell JA. 1989. A new method for preparation of undecalcified bone sections. *Stain Technol* 64:201–205.
- Sternberg CM. 1950. *Pachyrhinosaurus canadensis*, representing a new family of the Ceratopsia, from southern Alberta. *Bull Nat Mus Can* 118:109–120.
- Tanke DH, Farke AA. 2006. Bone resorption, bone lesions, and extracranial fenestrae in ceratopsid dinosaurs: a preliminary assessment. In: Carpenter K, editor. *Horns and Beaks*. Bloomington: Indiana University Press.
- Vickaryous MK, Russell AP, Currie PJ. 2001. Cranial ornamentation of ankylosaurs (Ornithischia: Thyreophora): reappraisal of developmental hypotheses. In: Carpenter K, editor. *The armored dinosaurs*. Bloomington: Indiana University Press.
- Wang X, Hoffman RS. 1987. *Pseudois nayaur* and *Pseudois schaeferi*. *Mamm Species* 278:1–6.
- Weinberg PJ. 2002. *Capra cylindricornis*. *Mamm Species* 695:1–9.
- West-Eberhard MJ. 1983. Sexual selection, social competition, and speciation. *Quart Rev Biol* 58:155–183.
- Witmer LM. 1995. The extant phylogenetic bracket and the importance of reconstructing soft tissues in fossils. In: Thomason J, editor. *Functional morphology in vertebrate paleontology*. Cambridge: Cambridge University Press. p 19–33.